Volume n° 2 - from B16 to B33

32nd INTERNATIONAL GEOLOGICAL CONGRESS

ULTRAHIGH AND HIGH PRESSURE ROCKS OF SAXONY

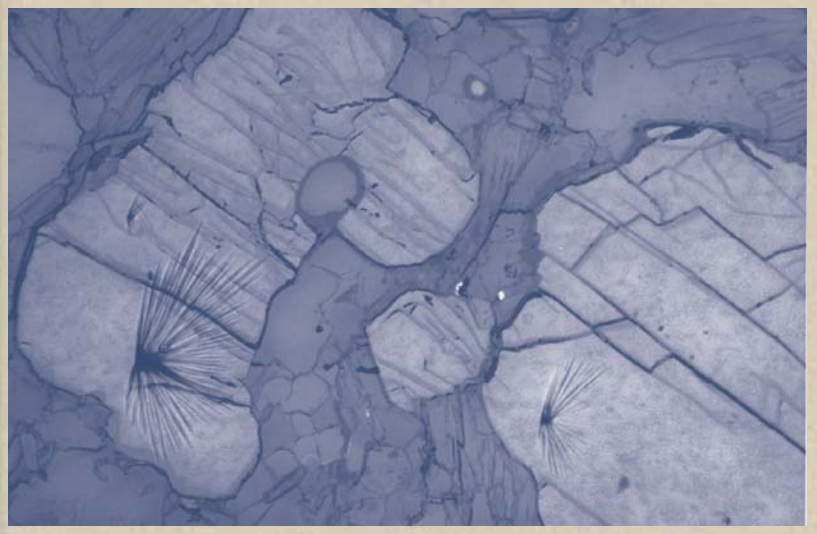

Leader: H.-J. Massonne

Associate Leader: H.-J. Bautsch

Field Trip Guide Book - B21

Florence - Italy
August 20-28, 2004

Pre-Congress B21

The scientific content of this guide is under the total responsibility of the Authors

Published by:
APAT – Italian Agency for the Environmental Protection and Technical Services - Via Vitaliano Brancati, 48 - 00144 Roma - Italy

APAT
Italian Agency for Environment Protection and Technical Services

Series Editors:
Luca Guerrieri, Irene Rischia and Leonello Serva (APAT, Roma)

English Desk-copy Editors:
Paul Mazza (Università di Firenze), Jessica Ann Thonn (Università di Firenze), Nathalie Marléne Adams (Università di Firenze), Miriam Friedman (Università di Firenze), Kate Eadie (Freelance indipendent professional)

Field Trip Committee:
Leonello Serva (APAT, Roma), Alessandro Michetti (Università dell'Insubria, Como), Giulio Pavia (Università di Torino), Raffaele Pignone (Servizio Geologico Regione Emilia-Romagna, Bologna) and Riccardo Polino (CNR, Torino)

Acknowledgments:
The 32nd IGC Organizing Committee is grateful to Roberto Pompili and Elisa Brustia (APAT, Roma) for their collaboration in editing.

Graphic project:
Full snc - Firenze

Layout and press:
Lito Terrazzi srl - Firenze

Volume n° 2 - from B16 to B33

32nd INTERNATIONAL GEOLOGICAL CONGRESS

ULTRAHIGH AND HIGH PRESSURE ROCKS OF SAXONY

AUTHORS:
H.-J. Massonne (Universität Stuttgart - Germany)
H.-J. Bautsch (Humboldt Universität - Germany)

Florence - Italy
August 20-28, 2004

Pre-Congress

B21

Front Cover:
Microdiamonds in garnets from quartzofeldspathic rock (saidenbachite), outcropping at the Saidenbach reservoir, Saxonian Erzgebirge, seen under reflected light. Striations around the diamonds allow to detect them easily. Image width is 3mm.

Leader: H.-J. Massonne
Associate Leader: H.-J. Bautsch

Introduction

Ultrahigh pressure (UHP) metamorphic rocks were first detected in the western Alps through the indicator mineral coesite (Chopin, 1984). Soon after this detection it turned out that UHP rocks are more widespread than expected after the first find. Coesite was also recognised in rocks of the Norwegian Caledonides, the Dabie Shan in China and orogenic regions elsewhere (Chopin, 2003). Evidence for UHP metamorphism, proven by both indicator minerals and mineral equilibria, has been reported only recently from the Variscan orogen in Europe. Typically, this orogen resulted from continent-continent collision in Phanerozoic times as the previously mentioned orogens with UHP rocks.

In portions of the Bohemian Massif, which is situated on the northwestern edge of the Variscan orogenic chain (Fig. 1), occurrences of eclogites and garnet peridotites were recognised more than a century ago and subsequent detailed mapping has revealed several hundred mostly small bodies spread over a very large area. Hints at UHP metamorphism came from specific mineral compositions (Al in orthopyroxene) and considerations of mineral equilibria, for instance, related to the Al-celadonite component in phengite. More recently, the indicator minerals coesite (Massonne, 2001) and microdiamond (Massonne, 1999) were detected in eclogites and quartzofeldspathic rocks, respectively, from the Erzgebirge. In addition, lamellae of garnet and clinopyroxene in clinopyroxenite from the nearby Granulitgebirge are interpreted as exsolution of former majoritic garnet (Massonne and Bautsch, 2002).

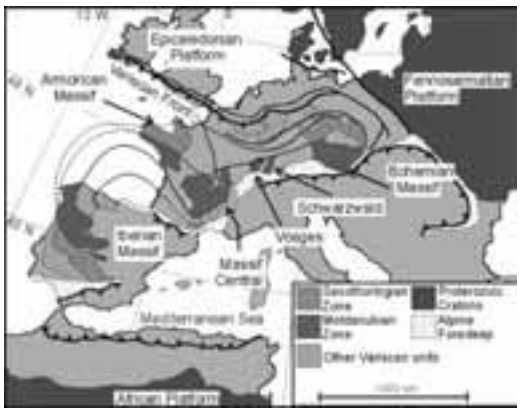

Figure 1 - Location of exposed basement areas of the Upper Palaeozoic Variscan orogen in Europe (Fig. 1 of O'Brien, 2000). These are subdivided in those belonging to the Saxothuringian Zone, Moldanubian Zone and other zones. Not shown are fragments of Variscan basement involved in the Cretaceous-Tertiary Alpine orogen.

The aim of our field trip is to present key occurrences of rocks formed at UHP and near-UHP conditions. These rocks are representative for high-pressure (HP) and UHP metamorphism in the Variscan orogen or at least in the Bohemian Massif. To gain detailed information on the regional geology we recommend having a look at the series of "Geologische Meßtischblätter". These maps with a 1: 25000 scale are distributed by "Sächsisches Landesamt für Umwelt und Geologie" at Dresden. In addition, explanatory text is available for each map. The following sheets cover the areas visited during our field trip: GK25 4943 Gehringswalde, GK25 4944 Waldheim, GK25 5042 Burgstädt, GK25 5043 Mittweida, GK25 5044 Frankenberg, GK25 5144 Flöha, GK25 5245 Lengefeld, GK25 5345 Zöblitz, and GK25 5543 Kurort Oberwiesenthal. Relevant overview maps with scale 1 : 200000 are GKÜ200 M33-VII Chemnitz, GKÜ200 M33-VIII Dresden, GKÜ200 M33-XIII Plauen, and GKÜ200 M33-XIV Annaberg-Buchholz.

Regional geology

It has become a common view that the Variscan orogen resulted from colliding continental plates. These were Gondwana and Laurentia-Baltica (or Laurussia). The latter were formed from originally separate plates during the Caledonian orogeny at the end of Early Palaeozoic times and, thus, shortly before the onset of Variscan events. It is assumed that after the end of the Caledonian orogeny (420-410 Ma) a single oceanic basin (Rheic ocean: e.g., Robardet et al., 1990; Tornquist Sea: Oliver et al., 1993) or two (e.g., Rheic ocean + Massif Central - Galician ocean, Matte, 1986; Rheic ocean + subsequently Palaeotethys, Stampfli et al., 2002) and more basins separated Gondwana and Laurentia-Baltica. The extension of the ocean(s) and the time of final closure is still a matter of debate (e.g., narrow: McKerrow et al., 2000; wide: Tait et al., 2000), which also includes the involvement of microplates, such as Armorica (see Tait et al., 1994: Armorican Terrane Assemblage), Avalonia (Murphy et al., 1999) or the Hun terrane (Stampfli, 1996), between Gondwana and Laurentia-Baltica. The many

Volume n° 2 - from B16 to B33

microplates were probably once contiguous to, or part of Gondwana (Tait et al., 2000; Hartz and Torsvik, 2002). In spite of the above uncertainties, the relative motion of Gondwana towards Laurentia-Baltica, implying the subduction of oceanic crust, is generally accepted. The subduction, also involving continental crust at a final stage, is assumed by many scientists to have been directed south or southeast (e.g., Franke and Stein, 2000) but the opposite direction is favoured by others (e.g., Matte, 1998). However, because of the bilateral symmetry of the structural elements of the Variscan orogen, two simultaneously active subduction zones with opposite directions, away from each other or even towards each other, were also taken into consideration by several geoscientists (e.g., Matte, 1986; Franke, 2000).

The basin of the Rheic ocean disappeared 340 Ma ago at the latest. However, attempts by some geoscientists to reconstruct the Variscan orogeny also consider a closure already about 400 Ma. Among such recent reconstructions, which also take into account the existence of HP and UHP rocks, is that by Matte (1998) proposing a process as suggested by the slab break-off model resulting in a relatively narrow mountain chain characterised by strongly thickened crust lasting for several tens of millions of years (Fig. 2). This also concerns the geodynamic model for the Variscan orogen presented by Massonne and O'Brien (2003) and Massonne (in press). However, these authors proposed underthrusting of one continental plate under the other to reach a Himalaya (+ Tibetan Plateau) type orogen by underplating during the course of several tens of millions of years (Fig. 3). After closure of the oceanic basin between Gondwana and Laurussia (called here: Rheic ocean) only small basins remained or were newly formed. In these, up to several km-thick sequences of Viséan and Upper Carboniferous sediments were deposited. Contemporaneously, large volumes of granitoid magmas intruded the Variscan crust.

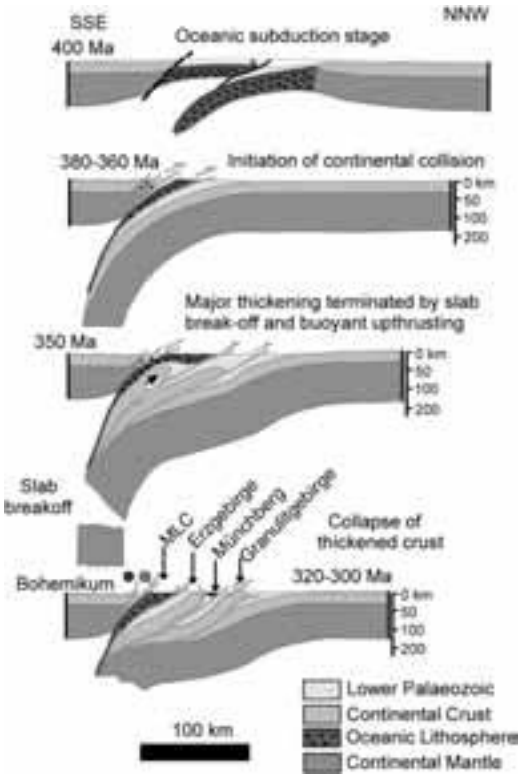

Figure 2 - The subduction-collision model by Matte (1998) redrawn by O'Brien (2000) for the northern Bohemian Massif.

The Bohemian Massif exposes the metamorphic core of the Variscan orogen at its eastern margin. It is a collage of several smaller basement areas differing in age and metamorphic evolution. These are termed Saxothuringian, Moldanubian, Tepla-Barrandian and in the east and northeast: Moravo-Silesian and Lugian = Sudetes (Fig. 4). Between the basement units, regions with Palaeozoic sediments exist that are predominantly only anchimetamorphic. Both sedimentary and metamorphic ages can be contemporaneous (e.g., Franke and Engel, 1986). Nappe tectonics (e.g., Schulmann et al., 1991) as well as major fault and shear zones (e.g., Krohe, 1996), which are widespread in the entire northern Variscan area, are responsible for the present collage-like aspect.

HP rocks in the Bohemian Massif, such as eclogites and garnet peridotites, are, in fact, abundant but are restricted to specific areas (dark in Fig. 4). As pointed out by Willner et al. (2000), the age data related to HP rocks are bimodal. Ages between 400 and 380 Ma, with up to 20 Ma younger cooling ages, were reported from the Münchberg Massif, the Góry Sowie (Owl Mountains) and the Tepla-Barrandian unit (Fig. 4). Clearly younger ages (345-340 Ma) were determined for HP rocks of the Granulitgebirge (Granulite Mountains), the Erzgebirge (Ore Mountains, Krušné hory in Czech), the Śnieżnik (Snowy Mountains) and the Gföhl unit. Cooling ages are on average only a few Ma younger. UHP rocks may occur in all units characterised by HP rocks but so far indicator minerals (see above) have only been found in the Erzgebirge.

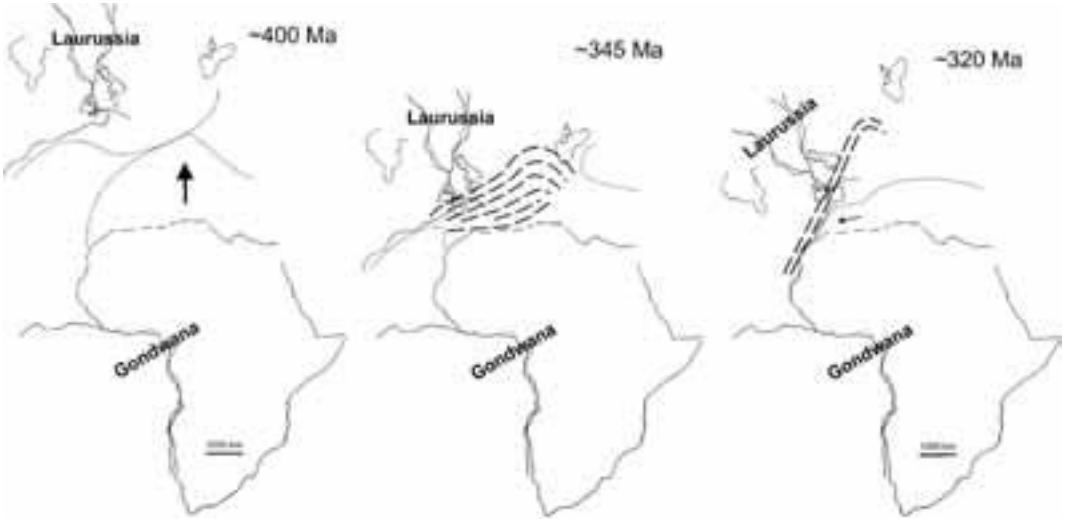

Figure 3 - Collision of Gondwana and Laurussia presented by the position of these continental plates relative to each other in the Lower Devonian (left hand side), Lower Carboniferous and Upper Carboniferous (right hand side) according to Massonne (in press). The positions of the plates refer to palaeomagnetic data (see Tait et al., 2000). For orientation the current shapes of the continental plates, except portions overprinted by the Alpine orogeny (see Northern Africa), and other typical geographic shapes (Hudson Bay, Newfoundland, Great Britain, Black Sea) are shown. The estimated shapes of the continental plates at the corresponding times are displayed by dotted lines (northern margin of Africa refers to pre-Alpine times). Thick dashed lines mark orogenic zones (= thickened continental crust). Arrows point

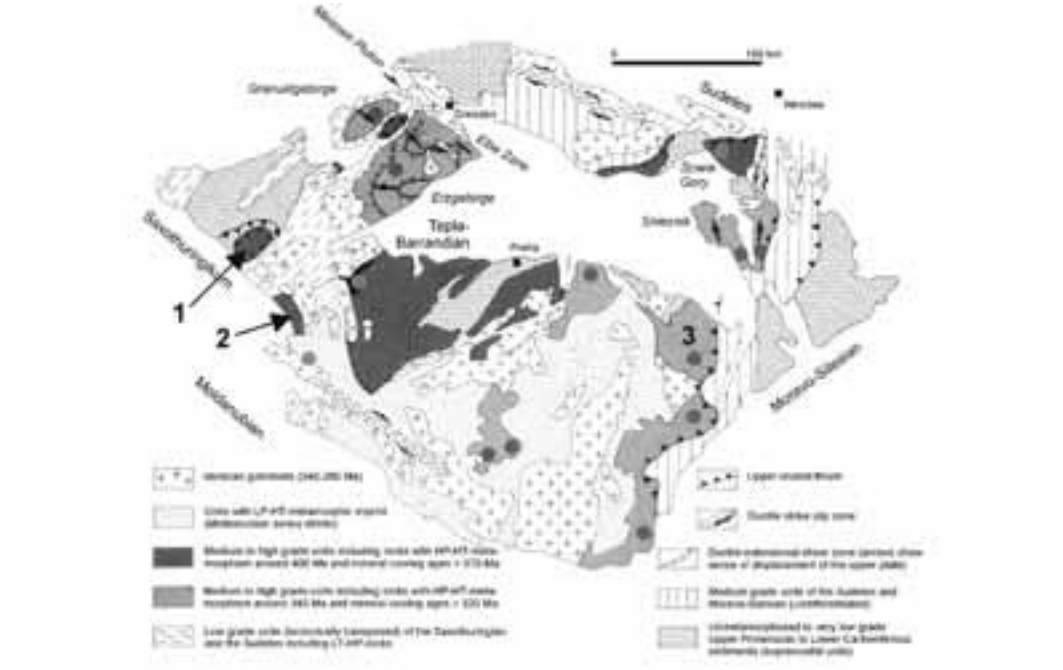

Figure 4 - Simplified geological map of the Bohemian Massif according to Willner et al. (2000). In addition to major units, specific areas are named (italics and 1 = Münchberg Massif, 2 = Zone of Erbendorf-Vohenstrauß, 3 = Gföhl Unit). Grey dots point to locations with HP rocks geochronologically dated.

Volume n° 2 - from B16 to B33

The crystalline complexes of both Granulitgebirge and Erzgebirge are anticlinal structures with ellipsoidal shape extending in WSW-ENE direction (Fig. 5). They are surrounded and, thus, covered by anchimetamorphic to low-grade metamorphic rocks. The outcropping rocks in the Granulitgebirge are either felsic and basic granulites with some ultrabasic bodies or younger granitoids (Fig. 5), whereas the rocks in the Erzgebirge are more variable in terms of metamorphic degree. Various suggestions exist to subdivide the metamorphic rocks. Here, we prefer the proposal by Willner et al. (2000) who suggested three major units for the medium to high-grade metamorphic rocks surrounded by a low-grade unit, the Phyllite Unit. Two of these three units, Mica-schist - Eclogite Unit (MEU) and Gneiss - Eclogite Unit (GEU), contain abundant eclogite lenses, whereas the Red and Grey Gneiss Unit does not contain any HP rocks. Detailed information on the P-T conditions of these units will be given in specific text portions related to corresponding rocks. This also refers to the Granulitgebirge. However, in general, it can be pointed out that the age of the HP metamorphism in both Granulitgebirge and Erzgebirge is close to 340 Ma (e.g. Massonne & O'Brien, 2003).

Figure 5 - Simplified geological map for the region of the Granulitgebirge (SGG) and the Erzgebirge (EZ) according to Blümel (1995). Vertically hatched - orthogneisses of the EZ, triangles - occurrences of larger eclogite bodies, crosses - granite bodies of Eibenstock, Bergen, and Schneeberg, swung dashes - phyllites surrounding the SGG, horizontally hatched - granitoid bodies in the SGG, black - serpentinite bodies. Abbreviations: FZ = Frankenberger Zwischengebirge, E.Z.R.F. = Erzgebirgssüdrand fault, D = Germany, CR = Czech Republic, CHEM = Chemnitz, DRE = Dresden, Fr. = Freiberg, O.W. = Oberwiesenthal, Rei. = Reitzenhain, Sa. = Sayda, W. = Waldheim.

Field itinerary

The field itinerary is subdivided into 4 portions according to the number of field trip days. The overview map at the back of the guide book shows the position of the various stops.

DAY 1

The route of the excursion starts in the city of Dresden towards the nearest access to Highway A4. Heading for Chemnitz on this highway, we leave it at exit 72 Frankenberg. After heading a few hundred metres towards Frankenberg, we turn right before reaching the inner town and cross the highway with an underpass. After about 1.5 km north, we see ahead the old "Fischerschänke" inn. Instead of following the road curving to the right, we turn left and stop at the parking area nearby.

Stop 1.1:

The target of this stop is to show a typical example for the border regions of the crystalline massifs. In order to demonstrate this, we walk northwest from the parking area along a hiking trail close to the eastern banks of the Zschopau river (Fig. 6). Before starting, we have a look at the cliffs of massive greenschists on the main road below "Sachsenburg" castle. After crossing the building area of the former "Schlossmühle" we can see slates outcropping on the right hand side. For the next 1.5 km, it is obvious that the metamorphic degree of the psammopelitic rocks, containing some basic intercalations, increase dramatically. Close to the granulites the slates have turned to micaschists and finally to migmatitic rocks containing cordierite. The first appearance of granulites is marked by cliffs along

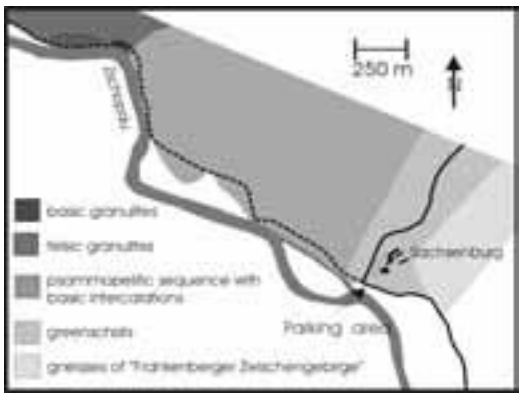

Figure 6 - Simplified geological map of the border zone at the south-eastern margin of the Granulitgebirge. The section shown is located in the Zschopau valley.

the hiking trail. These rocks are massive to platy and relatively fine-grained due to a mylonitic foliation. Felsic granulites are the dominant rock type there. They contain quartz, plagioclase, K-feldspar, minor garnet and kyanite. Biotite and amphibole seem to be retrograde phases of a medium temperature overprint. The intercalations and larger massive bodies of mafic

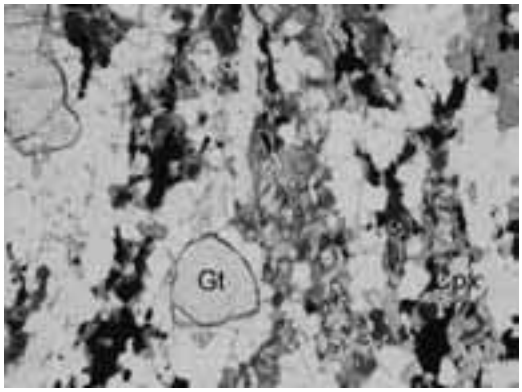

Figure 7 - Photomicrograph of basic granulite E301-3b. Plagioclase, amphibole, and ilmenite have formed at the expense of garnet (Gt), clinopyroxene (Cpx), and rutile. The latter phase is present as inclusion in garnet. Image width is 2 mm.

granulites are mainly formed from clinopyroxene, plagioclase, and garnet (Fig. 7). Minor constituents

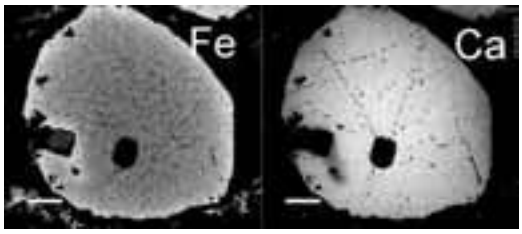

Figure 8 - Chemical zonation of garnet in basic granulite E301-3b. The grey code displays higher element concentrations by lighter tones. Scale bar represents 100 µm.

are orthopyroxene, rutile and quartz, which, however, can also be lacking. Amphibole, ilmenite and biotite are at least to some extent retrograde phases as in the felsic granulites. Orthoamphibole and chlorite can also occur as retrograde minerals.

Most minerals in the granulites are slightly zoned, thus, allowing estimations on the P-T evolution. For instance, garnet typically shows fairly homogeneously composed cores. Rims can be significantly poorer in Ca and Mg as well as richer in Fe (see Fig. 8 and Table 1). This chemical change follows the grain boundaries and is, thus, very likely due to a diffusional process at high temperatures. Clinopyroxene compositions tend to show decreasing jadeite contents towards the rim. For the granulites minimum P-T conditions were estimated to be 10 kbar and 800°C. It is not unlikely that the original

	Gt core	Gt rim	Cpx core	Cpx rim	Plag	Ilmenite	Amph	Amph	Biotite
	1321/12	1306/25	1306/15	1321/29	1319/5	1306/21	1320/19	1321/4	1320/3
SiO_2	38.76	37.78	50.43	51.60	60.05		44.19	40.53	35.63
TiO_2	0.16	0.08	0.43	0.25		51.93	1.96	2.70	3.32
Al_2O_3	21.38	20.92	3.35	2.12	26.21	0.07	9.97	14.51	14.19
Cr_2O_3	0.00	0.06	0.03	0.08		0.01	0.07	0.01	0.00
FeO	24.44	27.46	12.01	11.73	0.39	46.15	16.36	13.66	20.22
MnO	0.46	0.80	0.19	0.12		0.61	0.15	0.09	0.04
MgO	6.40	5.34	11.13	12.53		0.02	10.85	10.52	11.34
CaO	8.98	6.42	20.97	20.76	7.91	0.04	11.19	11.22	0.04
Na_2O			0.66	0.35	6.76		1.24	1.58	0.10
K_2O					0.29		0.92	2.20	8.89
Total	100.57	98.86	99.34	99.53	101.61	98.83	96.90	*97.13	*95.40
Si	5.947	5.980	1.917	1.950	2.637		6.570	6.067	5.535
Al^{IV}			0.083	0.050	1.356	0.002	1.430	1.933	2.465
Ti	0.018	0.010	0.012	0.007		0.997	0.220	0.304	0.388
Al^{VI}	3.866	3.902	0.067	0.044		0.002	0.316	0.627	0.132
Cr	0.000	0.008	0.001	0.002		0.000	0.008	0.001	0.000
Fe^{3+}	0.134	0.090	0.040	0.015	0.014		0.570	0.208	
Fe^{2+}	3.002	3.545	0.342	0.356		0.985	1.463	1.502	2.626
Mn	0.059	0.107	0.006	0.004		0.013	0.020	0.012	0.006
Mg	1.463	1.259	0.630	0.706		0.001	2.404	2.347	2.625
Ca	1.476	1.089	0.853	0.841	0.372	0.001	1.783	1.800	0.006
Na			0.049	0.025	0.575		0.357	0.458	0.029
K+Ba					0.016		0.174	0.426	1.861

*Table 1 - EMP analyses (in wt.%) of minerals from basic granulite E301-3b taken at the southeastern margin of the Granulitgebirge (Zschopau valley). *= total contains 0.11 wt.% (Amph) and 1.63 wt.% (Biotite) of BaO.*

Volume n° 2 - from B16 to B33

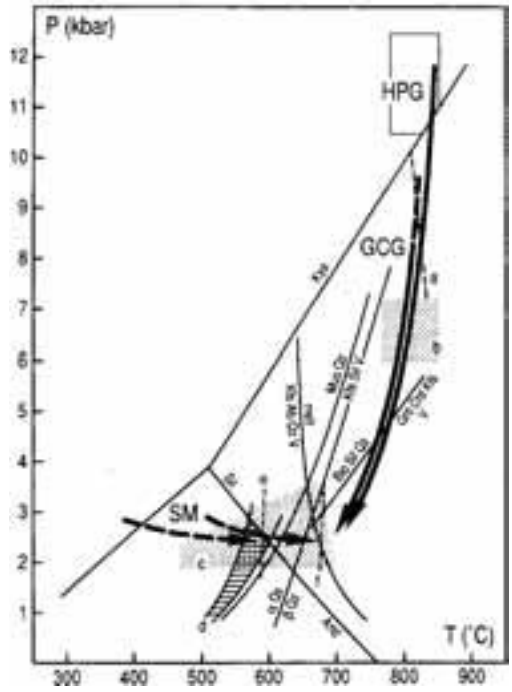

Figure 9 - P-T paths for the high pressure granulites (HPG) and the schist mantle (SM) of the Granulitgebirge according to Reinhardt and Kleemann (1994).

metamorphic conditions were significantly higher.

The retrograde alteration happened mainly during a strong pressure release at temperatures still above 700°C (see Fig. 9). On the contrary, the phyllite mantle as the hanging wall of the Granulitgebirge was drastically heated close to the contact to the granulites. This event occurred at depths of only 10 km (~ 3 kbar). According to strain indicators in the mantle rocks an extensional environment was suggested by Reinhardt and Kleemann (1994) as a cause for the final emplacement of a large fragment of lower crust, the Granulitgebirge, in such shallow crustal levels.

After returning to the parking area near the inn "Fischerschänke", we move back to Frankenberg. Again just before reaching the town, we turn left following route B169 heading for Hainichen and Döbeln. After about 11 km we cross Highway A4 and drive for an additional 4 km until reaching Greifendorf. Close to the centre of this village, we turn right to move along the banks of a brook for about 400 m. We stop at the road to then walk for about 150 m upwards to the entrance of an abandoned

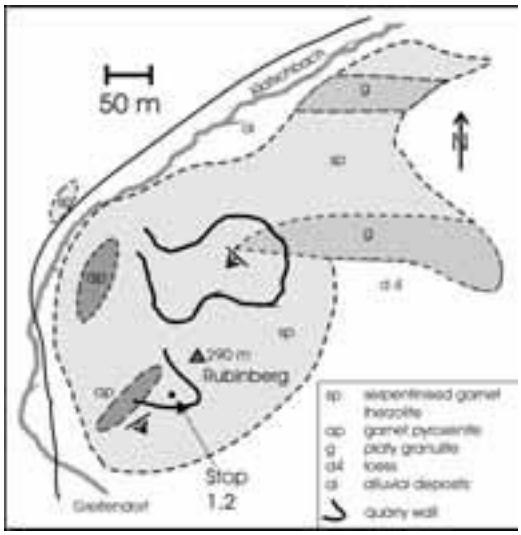

Figure 10 - Simplified geological map of the Rubinberg area, south-eastern Granulitgebirge.

quarry at Rubinberg hill (Fig. 10).

Stop 1.2:

The target of this stop is to show typical serpentinites of the Granulitgebirge, former garnet lherzolites, including pyroxenite bodies in these rocks. At the Rubinberg one can easily find serpentinites with relics of the mineral assemblage (Fig. 11) of a former lherzolite body that extends from the quarry of stop 1.2 to the northeast by about 3 km. From the partially conserved lherzolites one can reconstruct the fabric

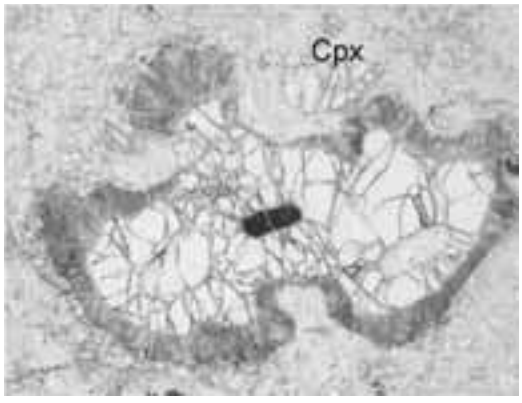

Figure 11 - Photomicrograph of a marginally altered garnet with decomposed inclusion minerals. The garnet is in serpentinised lherzolite GR99-1B. A larger relic of clinopyroxene (Cpx) is discernible nearby. Smaller relics of olivine and orthopyroxene are also present. Image width is 3.5 mm.

	Gt core 4-1B	Gt rim 1-1B	Cpx 16-1B	Cpx rim 29-1B	Opx 26-1B	Ol 18-1B
SiO_2	42.24	42.41	53.62	52.61	56.60	40.54
TiO_2	0.31	0.36	0.48	0.60	0.09	0.02
Al_2O_3	23.09	22.38	4.46	6.39	2.99	0.00
V_2O_3	0.03	0.04	0.06	0.08	0.01	0.00
Cr_2O_3	0.68	1.39	1.22	0.86	0.29	0.01
FeO	8.61	9.32	2.86	2.76	6.88	9.94
MnO	0.37	0.34	0.05	0.10	0.14	0.13
MgO	20.98	20.91	15.52	14.77	33.93	49.18
NiO			0.09	0.01	0.08	0.42
CaO	4.72	4.58	20.32	21.03	0.33	0.03
Na_2O	0.05	0.05	2.05	1.92	0.00	
K_2O			0.01	0.00	0.00	
Total	101.11	101.82	100.73	101.13	101.33	100.27
Si	5.889	5.909	1.929	1.886	1.932	0.992
Al^{IV}			0.071	0.114	0.069	0.000
Ti	0.033	0.038	0.013	0.016	0.002	0.000
Al^{VI}	3.795	3.676	0.118	0.157	0.052	
Cr	0.075	0.153	0.035	0.024	0.008	0.000
V	0.003	0.005	0.002	0.002	0.000	0.000
Fe^{3+}	0.127	0.167				0.016
Mg	4.360	4.344	0.832	0.789	1.726	1.793
Mn	0.044	0.040	0.002	0.003	0.004	0.003
Fe^{2+}	0.877	0.920	0.086	0.083	0.196	0.188
Ni			0.003	0.000	0.002	0.008
Ca	0.705	0.684	0.783	0.808	0.012	0.001
Na	0.014	0.013	0.143	0.134	0.000	
K			0.001	0.000		

Table 2 - EMP analyses (in wt.%) of minerals from serpentinised garnet lherzolite GR99-1B taken from the Rubinberg quarry, Granulitgebirge.

before serpentinisation. Garnets of several mm-size are in an equigranular matrix of significantly smaller clinopyroxene, orthopyroxene, and olivine. Together with the information on the chemical composition of the minerals (see Table 2) it is suggested that the relatively large, nearly homogeneous garnets belong to a pre-recrystallisation stage. Only the garnet rim adjusted chemically to the other silicates that were affected by deformation to recrystallise. In terms of relative pressure conditions, the chemical compositions are interpreted as follows. Garnet contains more Cr at the rim than in the extended core because of the breakdown of spinel as a result of pressure increase. Afterwards the matrix recrystallised. On the basis of geothermobarometry with garnet-clinopyroxene pairs as reported by Massonne and Bautsch (2002), P-T conditions close to 19 kbar and 1000°C can be derived for this stage. These data are compatible with the Al content in orthopyroxene associated with olivine and garnet. Subsequent pressure release is documented by increasing Al in clinopyroxene from core to rim.

Additional information on the P-T evolution

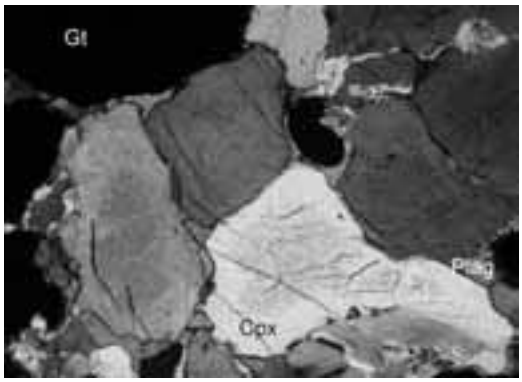

Figure 12 - Photomicrograph of an equigranular portion of sample GR99-1A rich in garnet (Gt) and clinopyroxene (Cpx). Plagioclase (Plag) and some amphibole occur along grain boundaries of garnet and pyroxene. Cpx contains numerous tiny inclusions of SiO_2 and alkalifeldspar all perfectly oriented. Image width is 1.5 mm.

comes from garnet-rich pyroxenite outcropping at the south-western wall of the quarry. This rock contains mainly mm-sized, equigranular garnet and clinopyroxene. However, rare cm-sized garnet can be detected as well. The large garnets are interpreted, similar to garnet in the lherzolite, as pre-recrystallisation mineral. Some plagioclase and rare amphibole have formed along grain boundaries mainly of clinopyroxene (Fig. 12). Small garnets seem to be also associated with plagioclase and amphibole. A process of partial melting is suggested also because of the irregular shape of garnet and the estimated temperature of about 1100°C for the rim compositions of garnet and clinopyroxene (Table 3). The corresponding pressure amounts to 22 kbar. Core compositions yielded somewhat higher temperatures at pressures of 26 kbar. At this stage the rock was an eclogite as the jadeite content in clinopyroxene was above 20 mol% (Table 3). In the clinopyroxene cores numerous, tiny and transparent rods could be detected (Fig. 12). Compositional investigations suggest SiO_2 and alkalifeldspar as exsolution of clinopyroxene. This phenomenon was assigned to UHP metamorphism, for instance, by Dobrzhinetskaya et al. (2002). Pressures as high as 30 kbar result at least from EMP analyses of clinopyroxene using a strongly defocused electron beam to obtain integral analyses of clinopyroxene and exsolution minerals (Table 3).

Returning to B169 at Greifendorf we move to the right but leaving the federal road almost immediately afterwards to go to Reichenbach and further on to Waldheim. In the centre of the town of Waldheim we

Volume n° 2 - from B16 to B33

	Gt core 42-1A	Gt small 53-1A	Cpx in Gt 43-1A	Cpx integr. 8N-1A	Cpx 59-1A	Plag 56-1A	Ilm 31-1A
SiO_2	39.95	39.90	49.63	51.49	49.15	60.88	
TiO_2	0.19	0.13	0.79	0.60	1.03	0.03	56.16
Al_2O_3	22.69	22.65	11.24	11.27	9.84	24.76	0.00
V_2O_3	0.05	0.03	0.14	0.10	0.13		1.11
Cr_2O_3	0.02	0.03	0.03	0.03	0.06	0.00	0.01
FeO	16.59	17.97	5.94	6.13	6.78	0.21	36.87
MnO	0.29	0.43	0.06	0.06	0.04	0.00	0.31
MgO	10.05	11.69	10.22	10.20	11.63	0.00	7.26
CaO	11.56	8.20	18.27	17.25	19.47	5.93	
Na_2O	0.05	0.03	3.46	3.46	1.97	8.51	
K_2O			0.00	0.02	0.02	0.26	
Total	101.45	101.07	99.78	100.61	100.12	100.58	101.73
Si	5.843	5.834	1.819	1.859	1.806	2.697	
Al^{IV}			0.181	0.141	0.194	1.293	
Ti	0.021	0.015	0.022	0.016	0.029	0.001	0.993
Al^{VI}	3.911	3.902	0.304	0.339	0.232		0.000
Cr	0.003	0.003	0.001	0.001	0.002	0.000	0.000
V	0.006	0.003	0.004	0.003	0.004		0.021
Fe^{3+}	0.081	0.091				0.008	0.013
Mg	2.191	2.547	0.558	0.549	0.637	0.000	0.255
Mn	0.036	0.053	0.002	0.002	0.001	0.000	0.006
Fe^{2+}	1.948	2.106	0.182	0.185	0.209		0.712
Ca	1.811	1.285	0.717	0.667	0.767	0.282	
Na	0.013	0.009	0.246	0.242	0.140	0.731	
K			0.000	0.001	0.001	0.015	

Table 3 - EMP analyses (in wt.%) of minerals (integr. = host + exsolution) from garnet pyroxenite (eclogite) GR99 -1A taken from the Rubinberg quarry, Granulitgebirge.

cross Zschopau river to turn left following the river to the south for some hundred metres. The main road then turns west heading for Reinsdorf. At the entrance of this village, an almost abandoned quarry is located on the right-hand side.

Stop 1.3:

Here another large serpentinite body of the Granulitgebirge was or still is quarried for macadam and to produce an artificial construction stone called "Terrazzo". However, the quarry seems to be used now to slowly fill up with construction debris and other trash. In contrast to the massive serpentinite of stop 1.2, the serpentinite body here is significantly layered due to a penetrative deformation event. This layering is concordant to the foliation of the surrounding felsic granulites. The ultrabasic body is as thick as 100 m outcropping over a larger area (Fig. 13). Pyroxenites occur as layers, 10 to 50 cm thick, or boudins parallel to the layering of the serpentinite. Veins and larger bodies of granitoids crosscut the ultrabasic rocks.

The serpentinite consists of about 60% orthochrysotile forming a mesh-like fabric. The meshes are oriented with an axial symmetry similar

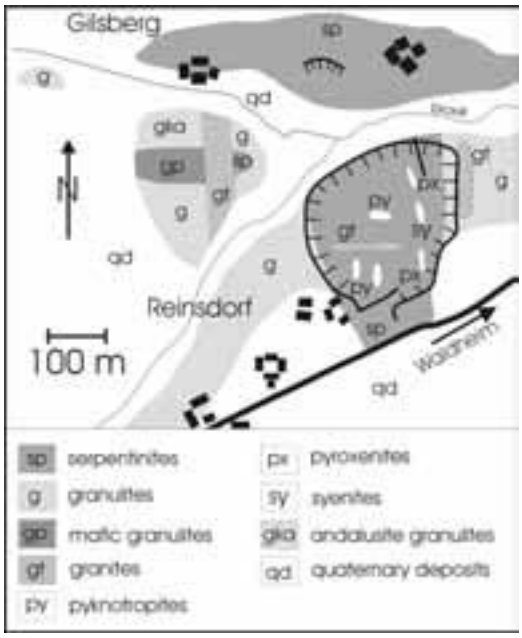

Figure 13 - Simplified geological map of an area east of the village of Reinsdorf, southeastern Granulitgebirge.

to the orientation of quartz c-axes in the nearby granulites. In addition to orthochrysotile, 20 to 30% lizardite occurs. Moreover, specific minerals such as carbonates appear close to the granitoids as a result of fluid-rock interaction. Originally, garnet was abundant but it is strongly altered. Nevertheless, pseudomorphs after garnet can be easily detected with the naked eye in many portions of the serpentinite body. However, very rare garnet up to 1 cm in size was found as well.

The pyroxenites can be subdivided into three groups. 1. Those consisting of garnet and clinopyroxene only; 2. clinopyroxenite with green spinel and garnet along the grain boundaries of coarse-grained clinopyroxene; 3. orthopyroxene-rich pyroxenite with some relics of megacrysts consisting now of thick lamellae of orthopyroxene and garnet. Type 1 pyroxenite can be collected along the eastern wall of the quarry whereas types 2 and 3 seem to have disappeared.

Portions of type 1 pyroxenite consist of parallel clinopyroxene (cpx) lamellae, which are fairly regularly spaced, as can be seen with the naked eye, and identically oriented since they display the same interference colour in a thin section under crossed nicols (Fig. 14A). X-ray studies by Reiche and Bautsch (1984) had confirmed this also for the garnet (gt) lamellae, which are topotaxially

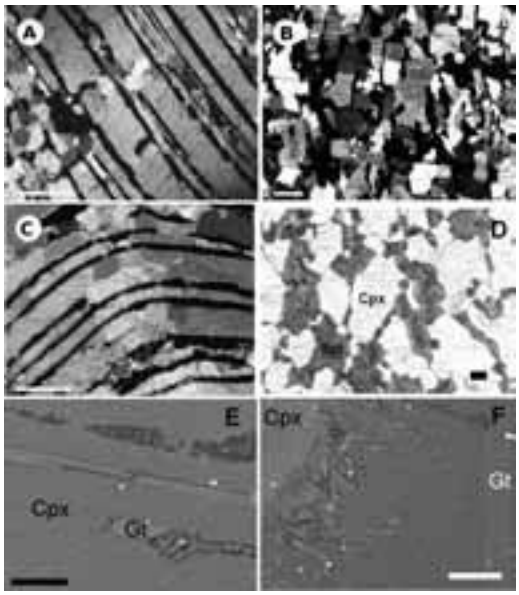

Figure 14 - Photomicrographs under crossed nicols (A-C) and under plain polarised light (D) as well as back scattered electron images (E,F) of pyroxenite types 1 (GR00-1: A-C) and 2 (PR 9457: D-F). Scale bars represent 1 mm (A-D) and 100 µm (E,F). The grey symplectites around spinel (Spi) in D have replaced garnet (Gt) at various stages as can be seen in F.

intergrown with clinopyroxene ((100)cpx//(110)gt and [001]cpx//[100]gt as well as (100)cpx//(100)gt and [001]cpx//[110]gt; Jekosch and Bautsch, 1991). As the lamellae can run parallel over cm, they were interpreted as former megacrysts (> 10 cm) with exsolution texture similar to those in pyroxenite type 3 (Reiche and Bautsch, 1985). The recrystallised fabric of equigranular garnet and clinopyroxene (Fig. 14B) close to the lamellae in pyroxenite type 1 is the result of deformation as we can see all kinds of transition from lamellar to equigranular fabric such as curved lamellae starting to recrystallise (Fig. 14C). Lamellar exsolution can also be observed in the mm-sized clinopyroxenes of type 2 pyroxenites. Here, formation of small garnet and more rarely spinel lamellae in clinopyroxene is obvious (Fig. 14E). But also the appearance of coarse grained garnet (and spinel?) along the grain boundaries of clinopyroxene is interpreted as reaction fabric (Fig. 14D). The orientation of clinopyroxene grains in pyroxenite types 1 and 2 is more or less isotropic whereas the recrystallised orthopyroxene grains in pyroxenite type 3, which frequently exhibit subgrain boundaries, are strongly oriented (Fig. 15). Finally, it is worthy of note that garnet can be replaced significantly

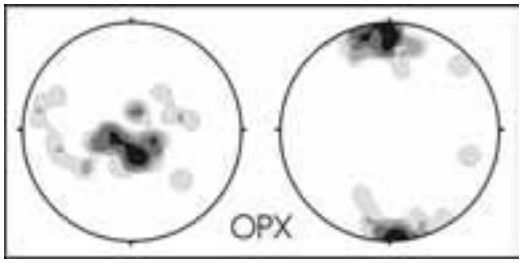

Figure 15 - Orientation of recrystallised orthopyroxene in type 3 pyroxenite (a-axes on the left, c-axes on the right hand side).

by various kinds of symplectites (Fig. 14F) often consisting of orthopyroxene and spinel but also of clinopyroxene, amphibole, potassic white mica and feldspars. The latter minerals are rather constituents of late alteration. Coarse-grained clinopyroxene is much rarer altered compared to garnet.

Electron microprobe analyses (Table 4) and element concentration maps (Figs. 16 and 17) show that garnet, clinopyroxene, and spinel in the clinopyroxenites are slightly non-homogeneously composed, thus, allowing to estimate various P-T conditions on the basis of the equilibria: (1) almandine (in gt) + 3 diopside (in cpx) = pyrope (in gt) + 3 hedenbergite (in cpx) and (2) 2 grossular (in gt) + pyrope (in gt) = 3 $CaAl_2SiO_6$ (in cpx) + 3 diopside (in cpx). For a sample of type 1 pyroxenite Massonne and Bautsch (2002) computed P-T data of about 25 kbar and 1000°C for an early stage due to formation of exsolution lamellae. Afterwards the mantle fragment was inserted into the lower portion of a thickened continental crust during the Variscan orogeny causing deformation and, thus, significant recrystallisation of the pyroxenite. This event was estimated to have happened close to 11

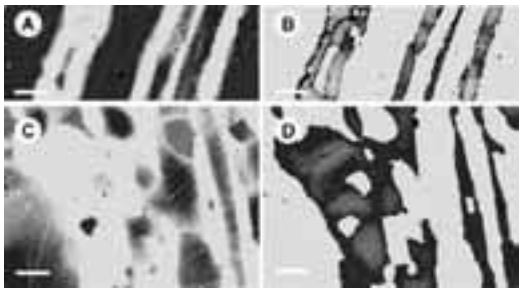

Figure 16 - Concentration maps of Al (left) and Ca (right hand side). A,B: Area (as in Fig. 14A) with lamellar microfabric of clinopyroxene and garnet (light in A and C). C,D: Strongly recrystallised area (as in Fig. 14B) close by. Lighter tones of the grey code refer to higher concentrations of the corresponding elements. Scale bars represent 200 µm.

Volume n° 2 - from B16 to B33

	PR 9457										GR 00-3			
	Gt1	Gt2	Gt3	Gt4	Cpx1	Cpx2	Cpx3	Cpx4	Spin1	Spin2	Gt1	Gt2	Cpx1	Cpx2
SiO_2	41.79	41.04	40.97	40.91	51.31	53.02	47.48	51.39	0.000	0.013	41.49	41.89	53.11	51.19
TiO_2	0.042	0.068	0.020	0.043	0.180	0.085	0.162	0.118	0.022	0.028	0.025	0.02	0.035	0.068
Al_2O_3	24.46	24.05	23.87	23.13	7.16	4.06	12.42	6.99	65.83	64.14	23.33	23.38	3.34	6.84
Cr_2O_3	0.184	0.180	0.208	0.472	0.087	0.063	0.068	0.085	2.25	1.74	0.295	0.295	0.171	0.212
V_2O_3	0.022	0.035	0.010	0.053	0.183	0.113	0.224	0.159	0.091	0.100	0.091	0.06	0.159	0.199
FeO	8.65	8.62	12.97	13.68	2.21	2.75	3.85	3.21	11.69	14.65	9.36	9.95	2.85	2.95
MnO	0.368	0.336	0.585	0.607	0.028	0.044	0.118	0.081	0.155	0.235	0.418	0.484	0.046	0.054
MgO	18.97	16.19	16.73	13.69	15.17	16.91	13.13	14.96	20.92	19.73	18.00	18.95	16.95	15.72
NiO				0.000				0.000	0.250	0.255	0.008	0.000	0.019	0.045
CaO	7.29	10.68	5.40	9.56	22.65	22.65	22.00	22.92	0.000	0.004	7.76	6.17	22.90	22.49
Na_2O	0.012	0.007	0.008	0.013	1.020	0.624	0.634	0.732			0.001	0.000	0.597	0.717
Total	101.80	101.22	100.78	102.07	99.99	100.28	100.02	100.62	100.99	100.91	100.78	101.19	100.18	100.47
Si	5.754	5.731	5.821	5.818	1.8591	1.9167	1.7308	1.8583	0.0000	0.0003	5.834	5.866	1.9185	1.843
Al^{IV}					0.1409	0.0833	0.2692	0.1417					0.0815	0.157
Ti	0.0043	0.0071	0.0021	0.0046	0.0049	0.0023	0.0044	0.0032	0.0004	0.0005	0.0026	0.0022	0.0010	0.0018
Al^{VI}	3.969	3.959	3.997	3.878	0.1649	0.0898	0.2645	0.1562	1.9276	1.9031	3.866	3.858	0.0610	0.1335
Cr	0.0200	0.0199	0.0234	0.0531	0.0052	0.0032	0.0065	0.0045	0.0442	0.0346	0.0328	0.0326	0.0049	0.006
V	0.0024	0.0039	0.0011	0.0060	0.0025	0.0018	0.0020	0.0025	0.0018	0.0020	0.0102	0.0068	0.0046	0.0057
Fe^{3+}	0.009	0.018	0.000	0.063					0.0255	0.0585	0.092	0.102	0.051	0.058
Fe^{2+}	0.987	0.989	1.541	1.564	0.0669	0.0831	0.1174	0.0970	0.2173	0.2500	1.010	1.062	0.035	0.031
Mn	0.0429	0.0397	0.0704	0.0731	0.0009	0.0013	0.0036	0.0025	0.0033	0.0050	0.0498	0.0574	0.0014	0.0016
Mg	3.892	3.370	3.544	2.902	0.8190	0.9110	0.7134	0.8063	0.7748	0.7406	3.770	3.956	0.9125	0.8435
Ni				0.0000				0.0000	0.0050	0.0052	0.0010	0.0000	0.0006	0.0013
Ca	1.076	1.598	0.822	1.457	0.8791	0.8773	0.8592	0.8881	0.0000	0.0001	1.168	0.926	0.8865	0.8675
Na	0.0024	0.0039	0.0011	0.0036	0.0717	0.0437	0.0448	0.0513			0.0002	0.0000	0.0420	0.0500

Gt1, Cpx1, Spin1 = core of coarse-grained garnet, clinopyroxene, and spinel, respectively; Gt2, Cpx2, Spin2 = corresponding rim compositions; Gt3, Gt4, Cpx3, Cpx4 = compositions of lamellae and blebs in coarse-grained Cpx.

Table 4 - EMP analyses (in wt.%) of minerals from pyroxenite types 1 (GR00-3) and 2 (PR 9457) in the serpentinite body at the village of Reinsdorf, Granulitgebirge.

kbar and 900°C. A more detailed P-T path could be derived from a type 2 pyroxenite (Massonne and Bautsch, 2003). This path (Fig. 18) shows a significant burial of the rock to depths of at least 100 km at temperatures above 1000°C during an early metamorphic stage. The subsequent exhumation path resembles that derived from type 1 pyroxenite. The late stage exhumation is compatible with the P-T path estimated for the granulites of the Granulitgebirge in general (see Fig. 9).

The bulk rock compositions of type 1 and 2 pyroxenites (Table 5) are not similar to those of common rocks such as gabbros. They rather reflect the composition of mono- to bimineralic layers as

Figure 17 - Concentration maps of Al and Ca of a section of sample PR 9457. The scale for the grey tones (increasing element concentrations towards the top) is on the right hand side. Scale bars represent 400 μm.

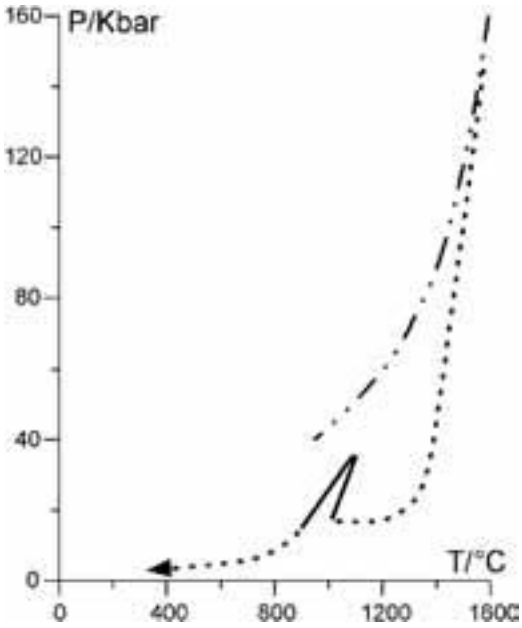

Figure 18 - P-T path (solid) derived for pyroxenites in the serpentinite body near the village of Reinsdorf, Granulitgebirge. The broken line of the path at UHP was inferred from geochemical studies (see text). The dashed-dotted curve represents the mantle geotherm.

Sample	PR9457	GR00-3L	GR00
Alteration in %	80	40	0
SiO_2 in wt.%	46.6	48.0	48.6
TiO_2	0.10	0.05	0.05
Al_2O_3	14.3	10.7	10.8
FeO	4.72	5.77	5.67
CaO	16.8	16.7	17.6
MgO	14.6	16.2	16.3
MnO	0.15	0.19	0.19
K_2O	0.38	0.20	0.00
Na_2O	0.28	0.48	0.50
P_2O_5	0.00	0.00	
H_2O_{tot}	0.59	0.45	
CO_2	0.26		
Sum	98.7	99.3	100.0
Li in ppm	84.5	31.8	22.5
Sc	91.5	112	112
V (XRF)	426	741	802
Cr (XRF)	1661	1247	1190
Ni	232	307	312
Cu	7.51	2.41	2.89
Zn	4.71	10.2	9.2
Ga	7.29	7.67	7.60
Rb	19.3	11.0	1.0
Sr	20.7	22.9	23.4
Y	11.0	8.92	9.3
Zr (XRF)	4	150	119
Nb	1.10	0.70	0.61
Sn	1.87		
Ba	45.8		< 20
Hf/Zr	b.d.l.	0.035	
Ta	1.44	0.70	0.55
Pb	0.04		
Th	b.d.l.	1.28	1.33
U	b.d.l.	0.89	0.90

Table 5 - XRF analyses of type 1 (GR00-3L) and type 2 (PR 9457) pyroxenites from the serpentinite body at the village of Reinsdorf, Granulitgebirge. The concentrations of most trace elements were determined by ICP-MS. GR00 shows values extrapolated to 0 % alteration using several analyses of similar rocks with various degrees of alteration. b.d.l.= below detection limit.

can be also inferred from the original megacryst nature at least of type 1 pyroxenites. On the basis of the REE patterns of the pyroxenites ($(Yb/Nd)_N$ > 10, Fig. 19), Massonne and Bautsch (2002, 2003) concluded that the pyroxenite layers originally consisted of majoritic garnets. For type 1 pyroxenite, such a garnet would have once contained about 50 mol% of $(Mg,Ca)_4Si_4O_{12}$ component. If this is true, the rock must have resided in the transition zone of the Earth's mantle (depths > 400 km). The uplift of the rock (for possible P-T path see Fig. 18) could have been facilitated by melts within a mantle plume. In the search for hints at such melts, boudins of quartz-free syenite, which are spatially related to the pyroxenites, were investigated (Massonne et al., 2002). However, the trace element pattern of the syenite showed no relation to ultrabasic rocks. It

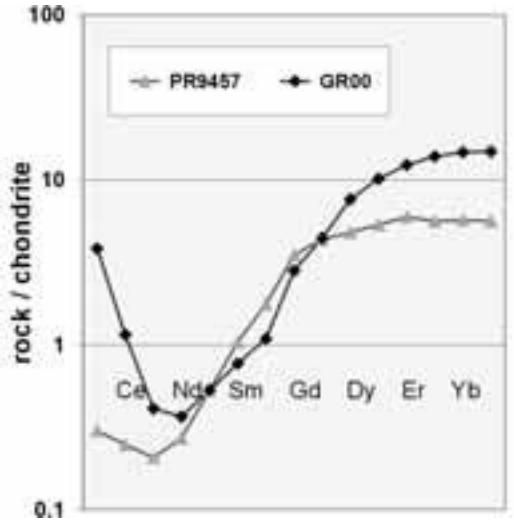

Figure 19 - REE pattern of clinopyroxenites occurring in the serpentinite body near the village of Reinsdorf, Granulitgebirge. The data were obtained by ICP-MS analyses and subsequently normalised to chondrite.

could be that the syenite was an ordinary felsic rock chemically altered by fluid-rock interactions with the serpentinite. This interpretation should hold true for the pyknotropites (see Fig. 13) which are former granitoids transformed to alkalifeldspar-rich rocks.

We return to Waldheim but stop soon after reaching the edge of town. We are now at the western banks of the Zschopau river. From here we walk southwards on a tourist trail along the river.

Stop 1.4: (optional)

Along the walk (see Fig. 20) cliffs appear on the right side of the tourist trail. Similarly, as seen during the walk of stop 1.1, we can discern felsic granulites as well as basic intercalations. It was about here where Rötzler and Romer (2001) discovered coarser grained metabasites and in them garnet with enclosed relics of omphacite. These authors used the original eclogitic nature of the rock to estimate early metamorphic P-T data. These were close to 1000°C and 22 kbar as also determined by Massonne and Bautsch (2002) for clinopyroxenites from the nearby village of Reinsdorf (see Fig. 18). Romer and Rötzler (2001) used the U-Pb system to determine the metamorphic event to 342 Ma. A very fast exhumation of the rock was deduced from almost identical U-Pb ages obtained from zircon, titanite, and apatite concentrates.

Volume n° 2 - from B16 to B33

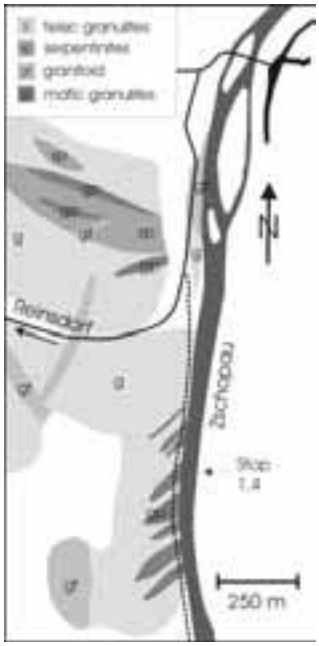

Figure 20 - Simplified geological map related to outcrops at the western banks of Zschopau river south of the town of Waldheim.

DAY 2

The route of the excursion continues from Waldheim to Hartha where we have access to federal road B175. We turn to the southwest heading for Rochlitz. Close to this town we change to federal road B107 heading for Chemnitz. After about 12 km, close to the entrance to Diethensdorf, we turn to the right passing this village by a relatively small road mostly going downhill. Just after crossing the Chemnitz river we turn at the road crossing to the right following the Chemnitz river valley to the northwest. After about a few hundred metres there are abundant parking lots on the left hand side and a large quarry, run by "Westsächsische Steinwerke", on the opposite side of the river.

Stop 2.1:

The target of this stop is to show again the typical felsic granulites of the Granulitgebirge but also ultrabasic and basic bodies in the felsic matrix. The extension of these bodies and their relation to the country rocks can be well investigated here because of the excellent exposure in the quarry (Fig. 21).

The felsic granulites consist mainly of quartz, plagioclase, K-feldspar, and some garnet. Relics of kyanite are discernible under the microscope (Fig. 22). More often, however, aggregates of sillimanite

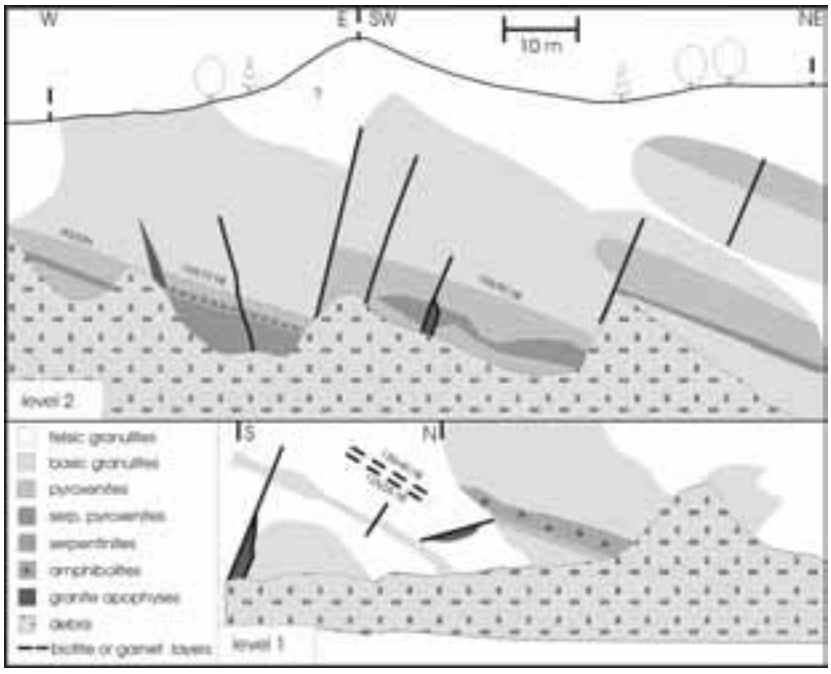

Figure 21 - Lithological relations seen at the walls of the large quarry in the Chemnitz valley close to the village of Diethensdorf, Granulitgebirge.

	Gt	Gt	Plag	Kf	Alkfs	Bt	Sill
	large core	small		small	with lamel.	small	
	2-8b	15-8b	13-8b	23-8c	25-8c	21-8c	19-8c
SiO_2	37.98	38.27	65.35	66.02	66.73	37.42	36.95
TiO_2	0.11	0.09	0.04	0.03	0.06	3.52	0.01
Al_2O_3	21.83	21.80	23.54	19.46	20.87	15.86	62.71
Cr_2O_3	0.01	0.03	0.00	0.01	0.01	0.05	0.00
FeO	29.16	30.76	0.09	0.03	0.01	13.58	0.56
MnO	0.50	0.61	0.00	0.00	0.03	0.01	0.01
MgO	6.71	8.16	0.00	0.01	0.00	14.59	0.02
CaO	4.23	1.02	3.90	0.05	1.10	0.00	0.01
Na_2O	0.00	0.00	8.39	1.01	4.77	0.19	0.01
K_2O			0.77	15.04	8.27	9.61	0.01
BaO			0.01	0.13	0.07	0.16	0.01
Total	100.53	100.77	102.09	101.79	101.92	94.98	100.32
Si	5.836	5.868	2.821	2.980	2.939	2.787	0.995
Al^{IV}			1.198	1.035	1.083	1.213	
Ti	0.013	0.010	0.001	0.001	0.002	0.197	0.000
Al^{VI}	3.954	3.940				0.179	1.990
Cr	0.002	0.004	0.000	0.000	0.000	0.003	0.000
Fe^{3+}	0.045	0.057	0.003	0.001	0.001		0.013
Mg	1.536	1.865	0.000	0.001	0.000	1.620	0.001
Fe^{2+}	3.703	3.889				0.846	
Mn	0.065	0.079	0.000	0.000	0.001	0.000	0.000
Ca	0.696	0.168	0.181	0.003	0.052	0.000	0.000
Na	0.000	0.000	0.702	0.088	0.407	0.027	0.001
K			0.042	0.866	0.465	0.913	
Ba			0.000	0.002	0.001	0.005	

Table 6 - EMP analyses (in wt.%) of minerals from the felsic granulite GR02-8c taken in the quarry at Diethensdorf, Granulitgebirge.

occur which have replaced kyanite. Biotite is probably a retrograde product only. Small portions of the rock contain mm-sized garnets being significantly larger than the ordinary garnets (Fig. 22). These portions seem to have been unaffected by the usual penetrative deformation that has led to fine-grained strongly foliated granulites. The composition of the extended cores of the large garnets differs significantly from that of their rims, which is nearly

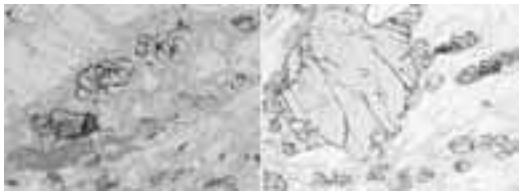

Figure 22 - Photomicrographs taken from felsic granulite sample GR02-8c (quarry close to Diethensdorf) under plain polarised light. Relics of kyanite (Ky) can be seen on the left hand side. Image width is 1.3 mm. On the right hand side, a large garnet (Gt) is discernible whereas garnets of common size in this rock are enriched in a layer below the big garnet. An aggregate of sillimanite (Sill) is a pseudomorph after kyanite. Image width is 2.5 mm.

	GR02-3c	GR02-7b	GR02-8b
SiO_2 in wt.%	43.97	43.59	46.28
TiO_2	1.29	1.34	0.46
Al_2O_3	16.30	16.82	10.30
Fe_2O_3	13.37	12.64	11.72
CaO	12.55	10.83	11.80
MgO	9.90	8.93	14.38
MnO	0.21	0.21	0.19
K_2O	0.10	0.45	0.01
Na_2O	1.47	1.89	0.96
P_2O_5	0.32	0.75	0.03
Sum	99.95	97.74	96.94
F	0.04	0.09	0.04
S	0.19	0.00	0.32
Cl	0.01	0.02	0.00
Sc in ppm	55	54	44
V	402	290	138
Cr	277	223	1416
Ni	113	113	1052
Cu	120	27	545
Zn	97	97	52
Ga	17	17	12
Rb	11	29	9
Sr	158	165	87
Y	24	39	26
Zr	58	93	298
Nb	9	13	0
Ba	210	134	3
La	12	27	3
Ce	86	95	23
Nd	16	40	6
Sm	5	7	3
Dy	5	7	2
Yb	6	5	12
Hf	4	4	3
Pb	4	8	1
Th	12	11	14
U	0	2	0

Table 7 - XRF analyses of garnet-rich pyroxenites from the Granulitgebirge.GR02-3c is from stop 1.2 (Rubinberg). GR02-7b was sampled close to stop 1.4 where railroad tracks are cut into the crystalline rocks a few hundred metres south of Waldheim station. GR02-8b is from the large quarry close to Diethensdorf (stop 2.1).

identical to the compositions of the small garnets (Table 6). Assuming 850°C and an anorthite activity of 0.2 in plagioclase (plag), the equilibrium: (3) grossular (in gt) + 2 kyanite + quartz = 3 anorthite (in plag) yields pressures as high as 17 kbar for the core composition of large garnets whereas pressures below 10 kbar result using the compositions of the small garnets.

The bulk compositions of garnet-rich pyroxenites associated with serpentinites were determined. Examples are given in Table 7. Whereas those from the Rubinberg quarry and from a body southwest of Waldheim (see Fig. 20) are, for instance, relatively rich in Ti, Al and light REE, the one in Table 7 from stop 2.1 is more similar to the garnet clinopyroxenites

Volume n° 2 - from B16 to B33

from the quarry at Reinsdorf. Relative high concentrations of Ni and Cu are here related to the presence of sulphides in the garnet pyroxenite.

We return to B107 passing Diethensdorf again. Then, we continue heading for Chemnitz but instead of passing the city of Chemnitz we take the alternative using Highway A4. We have access to A4 at the northern city limits heading for Dresden. After several km we leave the highway again at exit 72 Frankenberg. This time we are passing Frankenberg on its western side on B80 directed to Flöha. About 2 km after passing this town we turn left crossing Zschopau river in the village of Plaue. We continue heading for Augustusburg. If we want to go directly to stop 2.3 we have to turn left at a traffic light in the town, following the road sign to Leubsdorf, otherwise we keep going straight on for 150 m more. On the right-hand side there is a parking area for visitors.

Stop 2.2: (optional)

The famous castle of Augustusburg, erected by the Saxonian electors in only 4 years at the end of the 16th century, is settled on top of a remnant of a Permian rhyolitic lava flow. We recommend visiting a small abandoned quarry at the southeastern base of the castle hill by walking from the parking area about 200 m to the north (Fig. 23). The old quarry is somewhat hidden but close to the paved road leading to the castle. At the walls of the abandoned quarry the massive appearance of the reddish rhyolite can be

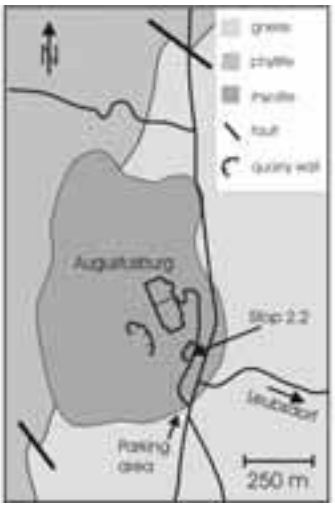

Figure 23 - Geological map showing the simplified relations of the Permian rhyolites to the crystalline basement around the town of Augustusburg, Saxonian Erzgebirge.

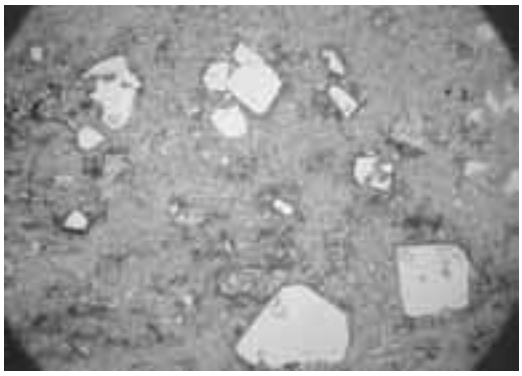

Figure 24 - Photomicrograph of a Permian rhyolite from Augustusburg containing phenocrysts of quartz and feldspars. Image width is 8.5 mm.

seen. The rock contains numerous quartz and feldspar phenocrysts (Fig. 24). A fluidal texture can also be easily recognised.

We return to the traffic light heading then towards Leubsdorf which we pass to follow the road to Eppendorf. Near the centre of this village we turn right into the road to Reifland then driving 1.6 km. A small road between houses appears on the left-hand side close to another road which turns to the right to Borstendorf.The road on the left leads us after 1.7 km to stop 2.3. We park ca. 50 m in front of another road our road leads to, because on the right-hand side there is a small abandoned quarry hidden in the forest.

Stop 2.3:

At this quarry we have a good exposure of massive eclogite belonging probably to a big lens or an assembly of several eclogite lenses (Fig. 25). In spite of the large eclogite bodies assumed to be below ground, further exposure of eclogite does not exist but abundant big blocks of eclogite can be found along the borders between fields and wood in the vicinity of stop 2.3. These blocks and the rocks in the quarry can contain fresh omphacite. However, this mineral can be completely altered to fine-grained symplectites of amphibole and plagioclase as well. Occasionally, omphacite + H_2O have reacted to form amphibole (Fig. 26) which could be as large as a few cm. This reaction still took place during the eclogite stage. The rare enrichment of potassic white mica might be also a reaction product of infiltrating H_2O when it contained potassium. Another interpretation of eclogitic layers rich in white mica is a pelitic protoliths originally present as thin strata within the basic rocks.

P-T conditions of the eclogite stage could be

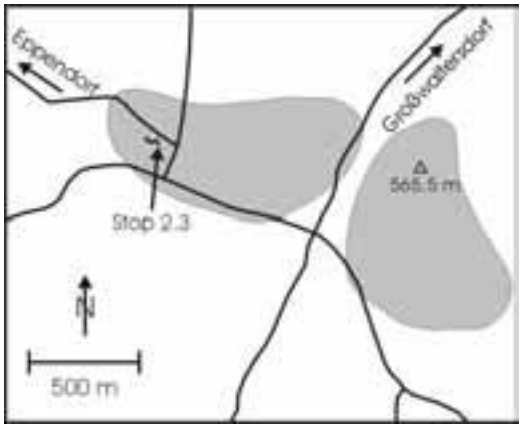

Figure 25 - Simplified geological map of an area in the GEU of the Saxonian Erzgebirge, southeast of Eppendorf, with large eclogite bodies (grey) embedded in gneiss.

determined from phengite-bearing eclogite which contained quartz, common as a minor constituent of the eclogites, and kyanite as a rare accessory phase in the eclogites. Mineral equilibria of geobarometric importance are here those using components in phengite (phe) as, for instance: (4) pyrope (in gt) + 2 grossular (in gt) + 3 Al-Mg-celadonite (in phe) = 6 diopside (in cpx) + 3 muscovite (in phe) and (5) 2 kyanite + grossular (in gt) + 3 Al-Mg-celadonite (in phe) = 3 diopside (in cpx) + 3 muscovite (in phe) + 2 quartz/coesite. In addition, the equilibrium: (6) muscovite + 2 rutile = 2 quartz + Ti-muscovite (= $KAl_3SiTi_2O_{10}(OH)_2$) can be applied because rutile is omnipresent in the eclogites. In the absence of phengite, the equilibrium: (7) 3 diopside (cpx) + 2 kyanite = pyrope (in gt) + grossular (in gt) + 2 quartz/coesite could be also used for metamorphic pressure estimation. As the minerals are moderately chemically zoned (Table 8) a small portion of the P-T path for the eclogite could be deciphered. Due to the significant decrease of Si in phengite this path is related to exhumation at maximum temperatures around 800°C (Massonne, 1994). The path starts at UHP conditions of somewhat more than 30 kbar ending close to 20 kbar and 700°C. UHP conditions are required for the occurrence of K-cymrite ($KAlSi_3O_8 \cdot H_2O$). According to Massonne et al.

	Gt		Omph		Phe	
	core	rim	core	rim	core	rim
	1109/09	1109/91	1109/80	1109/12	1109/33	1109/72
SiO_2	38.32	38.04	54.87	54.39	50.45	48.25
TiO_2	0.12	0.10	0.08	0.23	1.55	1.12
Al_2O_3	21.66	21.63	10.19	10.80	26.98	30.60
Cr_2O_3	0.01	0.04	0.00	0.03	0.02	0.01
FeO	21.07	20.96	4.63	4.25	1.28	1.29
MnO	0.38	0.43	0.00	0.07	0.00	0.00
MgO	5.65	6.13	8.81	9.03	4.01	2.71
CaO	13.12	11.85	15.21	15.76	0.00	0.00
BaO					0.18	0.11
Na_2O			5.40	5.33	0.47	0.83
K_2O					9.57	9.00
Total	100.33	99.19	99.36	99.88	94.51	93.93
Si	5.811	5.830	1.976	1.949	6.705	6.437
Al^{IV}			0.024	0.051	1.295	1.563
Ti	0.013	0.012	0.002	0.006	0.155	0.113
Al^{VI}	3.871	3.907	0.409	0.405	2.932	3.247
Cr	0.001	0.005	0.000	0.001	0.002	0.001
Fe^{3+}	0.128	0.088	0.000	0.003		
Fe^{2+}	2.544	2.598	0.139	0.125	0.142	0.144
Mn	0.049	0.056	0.000	0.002	0.000	0.000
Mg	1.277	1.400	0.473	0.483	0.795	0.539
Ca+Ba	2.131	1.946	0.587	0.605	0.010	0.006
Na			0.389	0.371	0.120	0.216
K					1.623	1.531

Table 8 - EMP analyses (in wt.%) of minerals from eclogite E174c taken from the large eclogite body SE of Eppendorf (stop 2.3), Saxonian Erzgebirge.

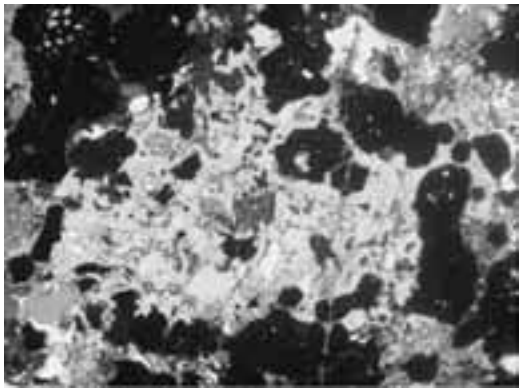

Figure 26 - Photomicrograph of an amphibole porphyroblast in eclogite sample Erz02-2 under crossed polarisers. The sample is from the quarry 2.5 km SE of the village of Eppendorf, Saxonian Erzgebirge. Image width is 4.5 mm.

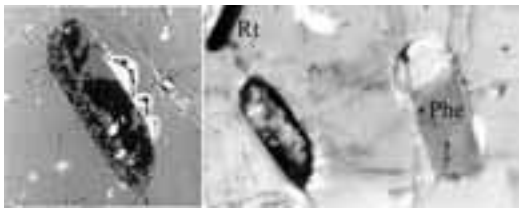

Figure 27 - Photomicrograph (right hand side) of inclusions (Rt = rutile, Phe = phengite) in omphacite of eclogite E174c (stop 2.3) under crossed polarisers. The inclusion (length about 140 µm) seen in the left corner at the bottom is also displayed as back-scattered electron image on the left hand side demonstrating the intergrowth of quartz and K-feldspar.

(2000), this mineral was enclosed in mineral cores mainly of omphacite but also in garnet. Now it is replaced by K-feldspar intergrown with quartz (Fig. 27). These pseudomorphs can be easily mistaken for those after coesite also because of cracks in the host mineral around the enclosed K-feldspar-quartz aggregate.

Results of geochemical analyses of eclogites from this locality and eclogite bodies nearby were reported by Massonne and Czambor (2003). These eclogites (SiO_2 = 48-52 wt.%, see Table 9) are characterised by $(Nb)_N$ = 5-36, $(Sr)_N$ = 5-17, Ta/Yb = 0.07-0.25, $(La/Sm)_N$ = 0.5-1.5, and $(Sm/Yb)_N$ < 1.8 (see Fig. 28). Massonne & Czambor (2003) referred these data to original MORBs. However, in addition to N-MORBs a trend to P-MORBs is discernible.

We take the road on the left heading for Großwaltersdorf. After passing this village we continue to Mittelsaida where we reach federal road B101. We turn left to drive ca. 19 km to the centre of Freiberg.

	1	2	3	4	5	6
SiO_2 in wt.%	49.76	49.93	51.58	51.25	49.50	50.29
TiO_2	1.88	2.06	1.32	1.54	1.92	1.67
Al_2O_3	15.78	15.60	16.47	16.14	14.80	16.70
FeO_{tot}	10.11	11.76	9.46	10.05	11.30	10.26
CaO	11.52	11.89	9.67	9.40	12.30	11.79
MgO	5.52	5.78	7.79	7.11	6.33	5.31
MnO	0.18	0.20	0.17	0.18	0.20	0.17
K_2O	0.09	0.09	0.13	0.38	0.23	0.40
Na_2O	2.78	2.39	2.52	2.62	2.32	2.48
P_2O_5	0.16	0.84	0.10	0.13	0.12	0.13
H_2O_{tot}	0.29	0.21	0.23	0.31	-	-
CO_2	0.16	0.12	0.05	0.15	-	-
Sum	98.23	100.87	99.49	99.26	99.02	99.20
Li in ppm	59.3	31.2	24.2	36.9	22.4	31.0
Sc	48.3	48.4	50.6	55.0	43.9	36.4
V (XRF)	326	365	225	236	353	336
Cr (XRF)	307	240	252	261	298	200
Ni	49.7	60.7	76.7	92.1	61.4	34.5
Cu (XRF)	80	57	16	26	69	89
Zn (XRF)	112	120	88	95	116	94
Ga	18.7	18.4	-	-	18.3	16.8
Rb	4.2	1.7	3.0	21.0	8.4	19.4
Sr	150	187	109	164	131	86
Y	60.1	59.0	24.2	24.5	39.7	31.8
Zr (XRF)	116	125	139	148	111	85
Nb	3.88	4.12	12.7	9.73	2.80	1.90
Sn	1.69	1.68	4.55	1.45	1.27	1.87
Ba (XRF)	56	31	71	61	42	274
Hf/Zr	0.043	0.054	0.028	0.034	0.032	0.040
Ta	1.17	0.74	1.01	0.76	0.34	0.26
Pb	3.33	2.10	4.35	2.37	1.59	1.45
Th	0.81	0.88	0.58	0.51	0.16	0.13
U	0.22	0.35	0.35	0.34	0.14	0.09

Table 9 - XRF and ICP-MS analyses of eclogites from the GEU of the Saxonian Erzgebirge. 1=Erz98-3 (at the village of Mittelsaida), 2=Erz98-4 (as 1), 3=KD39 (NE of the hamlet of Hutha), 4=KD59 (as 3), 5=E174c (stop 2.3), 6=E103c (1.2 km E of stop 2.3).

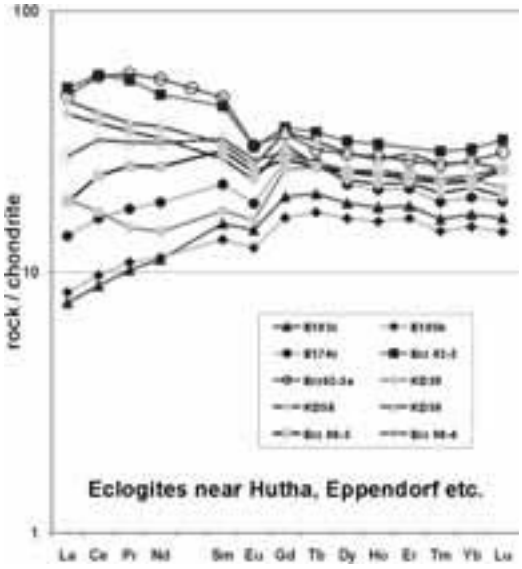

Figure 28 - REE patterns of eclogites in the northern to central portion of the GEU, Saxonian Erzgebirge. For localities see Table 9. The data were obtained by ICP-MS analyses and subsequently normalised to chondrite.

Stop 2.4:

At this stop we want to visit the mineralogical, petrological, and ore mineral collection of the Mining Academy at Freiberg. The museum is located in the town centre close to the dome erected in the 13th century. The Freiberg collections, founded in 1765, belong to the 10 oldest of currently more than 500 important geoscientific collections in the world. Especially the mineralogical collection is linked to famous names such as Werner, Mohs, Breithaupt, Weisbach, Kolbeck, and von Philipsborn. The exhibitions show a systematic mineral and rock collection, a regional collection of minerals and ore deposits of eastern Germany, specialities, for instance, related to precious stones and meteorites, and many more.

DAY 3

The route of the excursion continues from Freiberg to Annaberg-Buchholz. After about 23 km on B101 to the south we turn right at the entrance to the village of Forchheim heading for Lippersdorf. After 1.8 km we stop near the little bridge crossing the Saidenbach

brook. From here we have good access to the Saidenbach reservoir by walking on forest roads. As we want to visit first coesite-bearing eclogites at the northern shore of the reservoir (see Fig. 29), we take the trail on the north-western side of the brook. We walk for somewhat less than 2 km to reach the start of our tour along the shore of the reservoir provided that the water level is at least a few metres below maximum. However, this is usually so from July to September.

Stop 3.1A:

At this site we can easily find numerous blocks of eclogite along a 300 m section of the strand. Most of these blocks still contain fresh omphacite. The variety of eclogite here is surprising. Massive and foliated types exist as well as fine and coarser grained varieties. The eclogitic mineral assemblages are also variable. Rutile and quartz seem to be omnipresent. In a few cases, coesite could be detected in eclogite blocks from this locality (Massonne, 2001). However, it is only rarely preserved as inclusion in omphacite and garnet (Fig. 30) where it is then only partially transformed to quartz. Ba-rich potassic white micas with clearly decreasing Ba contents from core to rim were found in eclogite containing also cymrite but only as rare inclusion mineral (Table 10). Cl-rich apatite was reported by Massonne and Burchard (2000). This mineral, which is, untypical for apatite, significantly decomposed in the fresh eclogite, contained relative high amounts of Sr (> 4 wt.% SrO). Kyanite can be a rare constituent in eclogite blocks from this locality. Moreover, eclogites were found formed from conspicuous amounts of carbonate. Calcite, probably former aragonite, and dolomite can coexist in a single rock.

The bulk rock compositions of eclogites from stop 3.1A (Table 11) differ from those of MORBs. Instead of these rocks, magmatic protoliths related to oceanic islands, active continental margins or intraplate magmatism are conceivable. The REE patterns shown in Fig. 31 are compatible with such protoliths.

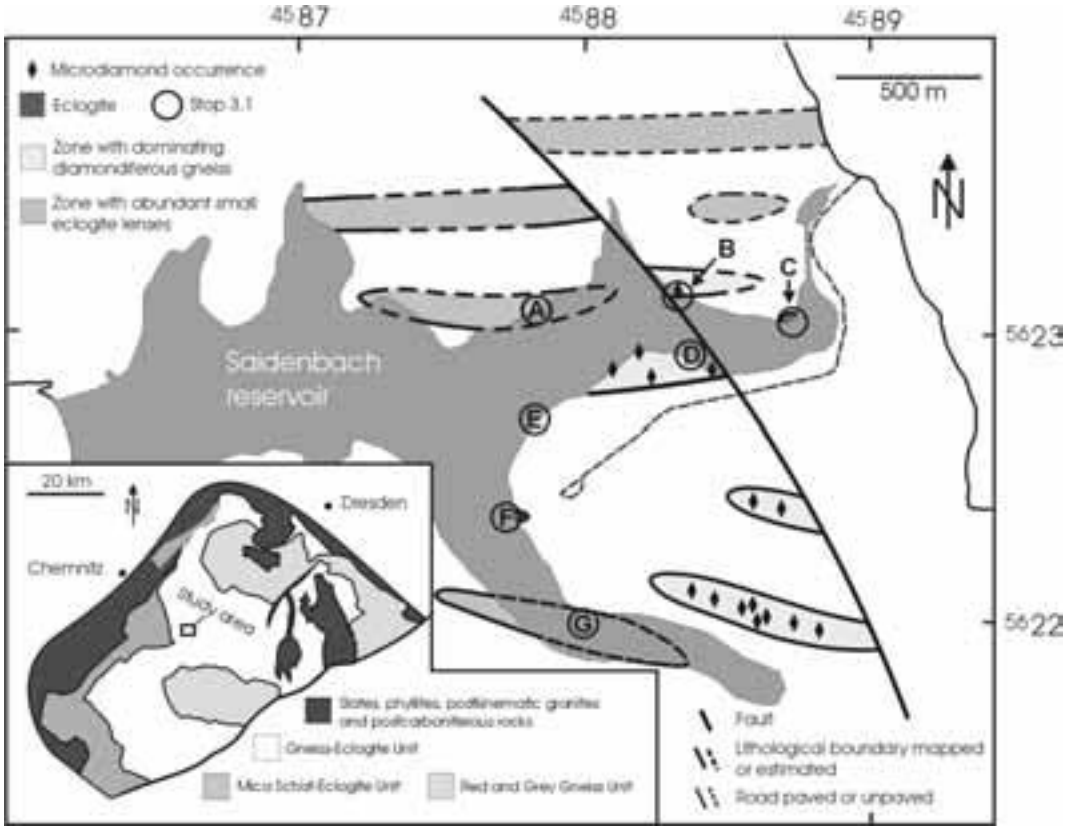

Figure 29 - Simplified geological map of the area around the Saidenbach reservoir. The map in the inlet shows the distribution of the GEU and MEU in the Saxonian Erzgebirge.

Table 10 - EMP analyses (in wt.%) of minerals in coesite-bearing eclogitic rocks from the Saidenbach reservoir, Saxonian Erzgebirge. Most analyses were taken from Massonne and Burchard (2000) and Massonne (2001). Structural formulae were calculated as given in Table 12 and as follows: cymrite - 16 valencies, carbonates - 2 cations without C.

Mineral	garnet	garnet	calcite	dolomite	kyanite	omphacite	phengite	K,Ba-mica	cymrite
Sample	E99-24	E99-24	E99-24	E99-24	E99-24	E99-24	E99-24	E99-23	E99-23
SiO_2	38.87	38.64	0.21	0.10	35.54	54.27	46.23	37.40	31.54
TiO_2	0.14	0.12	0.00	0.04	0.08	0.28	2.29	4.42	0.17
Al_2O_3	22.85	23.12	0.08	0.03	63.46	13.86	27.02	30.11	24.62
Cr_2O_3	0.02	0.09	0.06	0.04	0.06	0.06	0.09		
FeO_{tot}	12.40	15.35	1.71	3.30	0.34	2.57	1.41	0.85	0.31
MnO	0.20	0.36	0.05	0.09	0.03	0.04	0.08		
MgO	10.45	11.00	7.49	19.23	0.05	8.06	3.33	2.72	0.17
CaO	14.54	11.05	48.42	32.83	0.03	13.98	0.13	0.06	0.05
Na_2O	0.06	0.05	0.07	0.02	0.00	6.17	0.37	0.01	0.12
K_2O	0.03	0.00	0.03	0.00	0.00		10.48	5.06	0.28
BaO	0.05	0.09	0.08	0.00	0.01		0.72	14.51	39.79
Cl								0.10	0.81
Total	99.60	99.87	58.24	55.68	99.62	99.31	92.13	95.84	97.86
Si	5.650	5.617	0.006	0.003	0.962	1.938	6.473	5.632	2.044
Ti	0.015	0.013	0.000	0.001	0.002	0.008	0.241	0.501	0.008
Al	3.915	3.961	0.003	0.001	2.024	0.583	4.459	5.344	1.881
Cr	0.002	0.010	0.002	0.001	0.002	0.002	0.010		
Fe	1.507	1.866	0.044	0.082	0.008	0.077	0.185	0.107	0.017
Mn	0.025	0.044	0.001	0.002	0.001	0.001	0.010		
Mg	2.264	2.383	0.342	0.855	0.002	0.429	0.695	0.611	0.016
Ca	2.265	1.721	1.589	1.049	0.001	0.535	0.020	0.010	0.004
Na	0.017	0.014	0.004	0.001	0.000	0.427	0.100	0.178	0.015
K	0.006	0.000	0.001	0.000			1.672	0.972	0.023
Ba			0.001	0.000			0.040	0.856	1.010
Cl								0.026	0.089

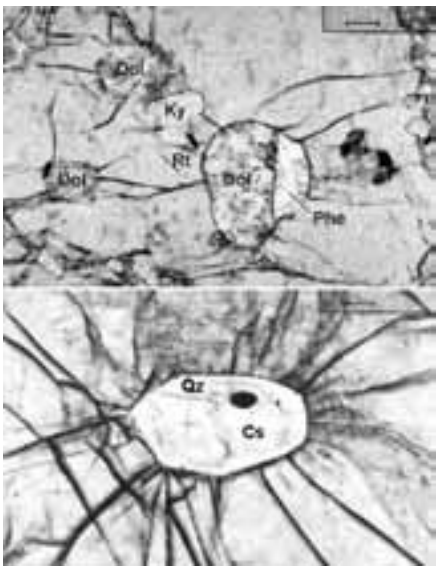

Figure 30 - Photomicrographs of inclusions (Dol= dolomite, Ky=kyanite, Phe=phengite, Rt=rutile) in garnet of eclogite sample E99-24 under plain polarised light. The sample is from stop 3.1A. Coesite (Cs) is surrounded by quartz (Qz). Image widths are 1.3 mm (at the top) and 0,65 mm (at the bottom).

W e

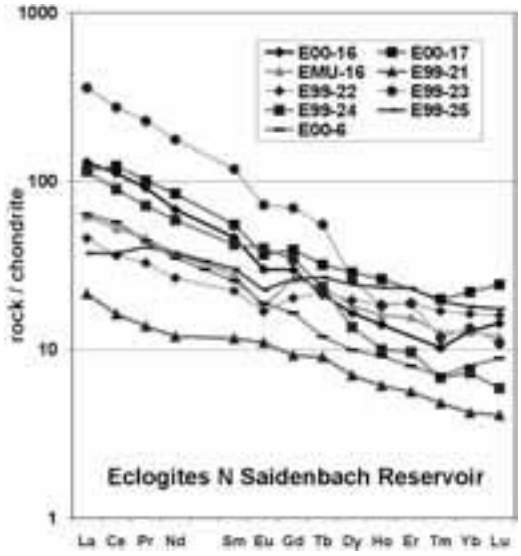

Figure 31 - REE patterns of eclogites from the northern shore of the Saidenbach reservoir (GEU, Saxonian Erzgebirge). The data were obtained by ICP-MS analyses and subsequently normalised to chondrite.

	E99-22	E99-23	E99-25	E00-6	E00-16	E00-17
SiO2 in wt.%	55.75	47.53	50.6	49.12	47.92	49.92
TiO2	1.66	0.85	3.37	1.22	1.06	3.07
Al2O3	15.60	17.63	15.28	16.55	16.66	16.23
FeOtot	8.94	7.08	12.35	7.97	9.37	12.44
CaO	7.44	10.08	8.34	12.84	10.41	8.26
MgO	4.24	8.79	4.29	8.42	7.84	4.03
MnO	0.14	0.11	0.20	0.14	0.15	0.20
K2O	1.54	0.96	0.78	0.41	0.41	0.51
Na2O	3.30	2.28	3.21	2.33	2.39	3.49
P2O5	0.15	0.22	0.79	0.15	0.16	0.84
H2Otot	0.82	0.36	0.57	0.25	0.23	0.22
CO2	0.12	0.34	0.10	0.25	0.41	0.11
Sum	99.90	96.23	99.88	99.65	97.33	99.34
Li in ppm	36.9	32.2	14.1	11.2	14.5	16.1
Sc	29.0	30.4	35.4	43.6	30.4	30.8
V (XRF)	214	138	317	227	193	317
Cr (XRF)	102	263	47	213	300	83
Ni	19.3	180	10.6	58.6	105	11.5
Cu (XRF)	22	72	37	81	81	30
Zn (XRF)	92	63	128	60	80	136
Ga	20.7	-	22.7	14.6	14.9	20.0
Rb	30.4	27.0	10.8	9.6	8.8	9.7
Sr	162	891	212	269	405	355
Y	29.8	16.8	37.1	18.7	29.5	55.0
Zr (XRF)	158	98	109	77	87	87
Nb	12.3	8.5	47.9	18.2	13.6	58.9
Sn	0.65	1.06	0.32	0.27	0.41	0.00
Ba (XRF)	306	2823	65	164	687	182
Hf/Zr	0.029	0.025	0.028	0.032	0.030	0.048
Ta	0.49	0.59	2.48	1.23	0.91	3.53
Pb	5.05	107	1.48	3.37	17.8	4.85
Th	3.97	18.2	0.07	4.48	5.43	3.63
U	0.27	4.41	0.04	0.89	1.29	0.60

Table 11 - XRF and ICP-MS analyses of eclogites from the northern shore of the Saidenbach reservoir, GEU of the Saxonian Erzgebirge.

move along the strand to the northeast. After crossing the issue of a little brook into the reservoir we walk for a few hundred metres to the southeast.

Stop 3.1B:

At this site we can recognise boulders differing from those of migmatitic gneisses ("Flammengneise") which appeared along the strand after we left the area with blocks of eclogites. These boulders consist of a non-foliated quartzofeldspathic rock with a homogeneous distribution of abundant mm-sized garnets. Muscovite forms a considerable portion of the matrix. Microdiamonds can be detected as inclusion in garnet and other phases (for details see stop 3.1D). Boulders of this rock, proposed to be named after the type locality saidenbachite (Massonne, 2003), occur very locally, so that this occurrence is interpreted as a lensoid body in the underground surrounded by migmatitic gneisses (see map of Fig. 29).

We continue to walk to the east for a few hundred metres and stop where the (former) Saidenbach brook changes direction.

Stop 3.1C:

At this corner, boulders of an eclogitic rock are concentrated. It seems to be that we can see here a real exposure of the rock. In contrast to the eclogites of stop 3.1A, this rock is homogeneous and non-foliated. Similar to the diamondiferous rock of stop 3.1B, mm-sized garnets are homogeneously distributed in the rock although the concentration of garnet is higher and the matrix is different compared to the rock of stop 3.1B. The matrix originally consisted mainly of phengite, quartz, and abundant omphacite. However the omphacite is entirely replaced by relatively coarse-grained symplectites of plagioclase and diopside-rich clinopyroxene or amphibole. Phengite is rarely completely but at least marginally substituted by biotite and plagioclase but also, probably during a late retrograde stage, by a fine-grained micaceous material. Microdiamonds could not be detected as inclusion mineral but omphacite rarely survived as inclusion in garnet (for more details see stop 3.1F).

We walk north to cross Saidenbach brook. Afterwards, we continue on the eastern strand heading south for several hundred metres and then to the west for several hundred metres more.

Stop 3.1D:

Again we meet with blocks of diamondiferous rocks seen before at stop 3.1B. Such blocks can be

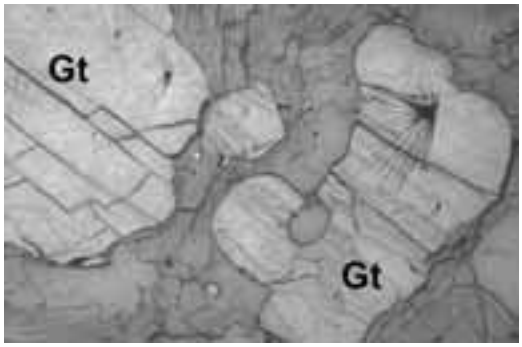

Figure 32 - Photomicrograph of microdiamonds enclosed in garnet (Gt) from quartzofeldspathic rock E97-3 seen under reflected light. Striations around the diamonds allow to detect them easily. Image width is 3 mm.

Mineral	garnet core	garnet core	garnet mediate	garnet rim	garnet incl. in zircon	jadeite incl. in zircon	kyanite	phengite core	phengite rim	phengite in garnet
Sample	S6100	E97-2	E97-2	E97-2	S6100	S6100	E97-2	E97-1	E97-1	S6100
SiO_2	38.80	38.57	38.66	39.00	39.07	58.54	36.66	47.90	47.15	49.67
TiO_2	0.075	0.203	0.133	0.053	0.018	0.264	0.007	2.11	2.32	3.32
Al_2O_3	22.59	22.20	22.32	22.34	22.44	22.80	63.19	28.64	29.70	28.25
Cr_2O_3	0.01	0.02	0.02	0.06	0.04	0.02	0.037	0.05	0.05	0.05
FeO_{tot}	26.02	26.06	26.11	25.32	24.93	1.72	0.084	1.48	1.54	1.11
MnO	0.39	0.34	0.34	0.295	0.25	0.00		0.00	0.03	0.06
MgO	9.59	7.57	8.26	8.33	10.18	2.28	0.046	2.97	2.59	3.51
CaO	3.57	5.50	4.40	5.22	3.44	3.04		0.02	0.01	0.01
Na_2O	0.13				0.08	11.95		0.27	0.23	0.72
K_2O	0.00				0.00	0.00		9.91	9.91	9.77
BaO								0.32	0.21	0.28
F								0.11	0.10	0.21
Total	101.17	100.46	100.24	100.62	100.44	100.63	100.08	93.79	93.83	96.97
Si	5.785	5.906	5.918	5.936	5.871	2.003	0.988	6.478	6.367	6.497
Ti	0.008	0.024	0.016	0.006	0.002	0.007	0.0014	0.215	0.235	0.327
Al	3.970	4.006	4.026	4.006	3.974	0.920	2.007	4.564	4.727	4.354
Cr	0.001	0.002	0.002	0.006	0.004	0.001	0.0008	0.005	0.005	0.005
Fe	3.245	3.338	3.342	3.220	3.133	0.049	0.0019	0.167	0.174	0.122
Mn	0.049	0.044	0.044	0.038	0.032			0.000	0.004	0.006
Mg	2.131	1.728	1.884	1.890	2.280	0.118	0.0019	0.598	0.521	0.685
Ca	0.570	0.902	0.720	0.850	0.554	0.111		0.000	0.000	0.001
Na	0.035				0.022	0.793		0.070	0.060	0.184
K								1.710	1.706	
Ba								0.017	0.011	
F	-							0.048	0.044	1.645

Table 12 - EMP analyses (in wt.%) of minerals in diamondiferous quartzofeldspathic rocks from the Saxonian Erzgebirge. The analyses were taken from Massonne (1999) as well as Massonne and Nasdala (2003). Structural formulae were calculated (as in previous and subsequent Tables) as follows: clinopyroxene (here: jadeite) - 4 cations, garnet - 10 six- and eightfold coordinated cations, kyanite - cation sum = 3, mica - 42 valencies without interlayer cations.

found for the next 500 metres continuing to walk westward. Thus, it is concluded that a larger body of diamondiferous quartzofeldspathic rock is subsurface. Detailed analytical studies of the mineral compositions (see Table 12) confirm that the microdiamonds (see Fig. 32) are enclosed in a specific compositional zone of garnet. This intermediate zone is characterized by low Ca concentrations (Fig. 33). Ca contents of the garnet core and the thin and irregular rim are higher. Micro-diamond inclusions in kyanite, which is, in general, a relic only as it is altered to white mica (Fig. 34), can occur in an intermediate zone as well. In the

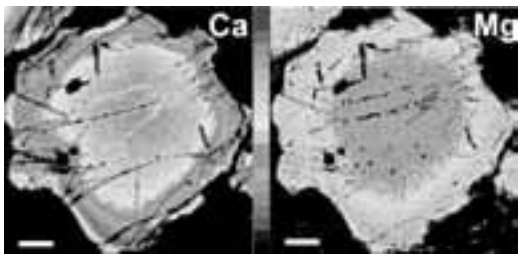

Figure 33 - Concentration maps of Ca and Mg of garnet in sample E97-2. The scale for the grey tones (increasing element concentrations towards the top) is in the middle. Scale bars represent 250 µm.

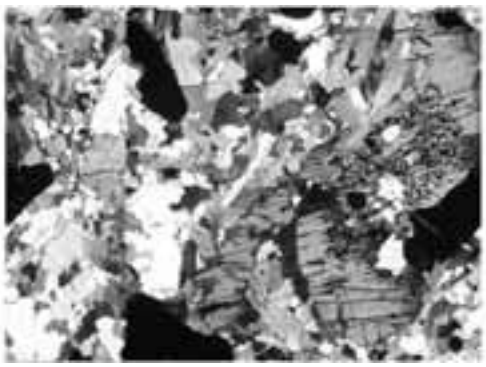

Figure 34 - Photomicrograph of a large kyanite from sample E97-3 seen under crossed nicols (Massonne, 2003). In the core of the crystal abundant small garnets are enclosed. Arrows point to microdiamonds. Image width is 4 mm.

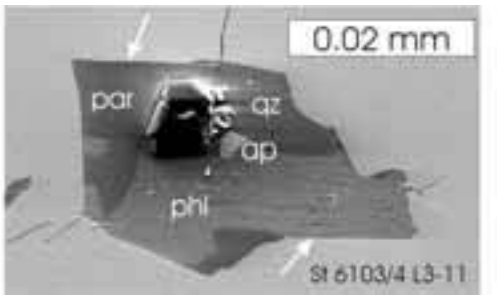

Figure 35 - SEM image of a polyphase diamond-bearing inclusion in garnet from quartzofeldspathic rock of the Saidenbach reservoir, central Saxonian Erzgebirge (Stöckhert et al., 2001). Arrows point to rational mica garnet interfaces. qz = quartz, par = paragonite, phl = phlogopite, ap = apatite.

kyanite core numerous small garnets are occasionally enclosed. Another interesting feature is the association of diverse minerals with diamond within a single inclusion in garnet (Fig. 35). Such minerals are quartz, feldspars, various micas, and occasionally apatite and rutile. Stöckhert et al. (2001) interpreted the polyphase inclusions as trapped siliceous fluid. In zircon, also containing microdiamonds (Nasdala and Massonne, 2000) in an intermediate growth zone, rare inclusions of garnet and jadeite were observed (Fig. 36). In addition, inclusions of phengite, quartz, and rutile occur in garnet cores. From these inclusion minerals, P-T conditions close to 18 kbar and 600°C were derived by geothermobarometry (Massonne and Nasdala, 2003). This result is almost identical to that by Willner et al. (1997) for gneisses in the vicinity of the saidenbachites. It was interpreted by Massonne and Nasdala (2003) as evidence for the location of the protolith of the saidenbachites at the base

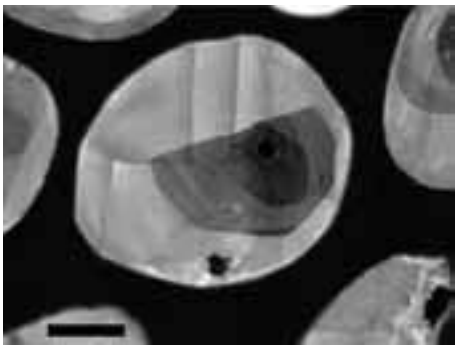

Figure 36 - Cathodoluminescence image of zircon from sample St6100. This mineral contains a jadeite inclusion (black) in the dark core zone. Microdiamond (black) appears in the lighter zone. Scale bar is 50 µm.

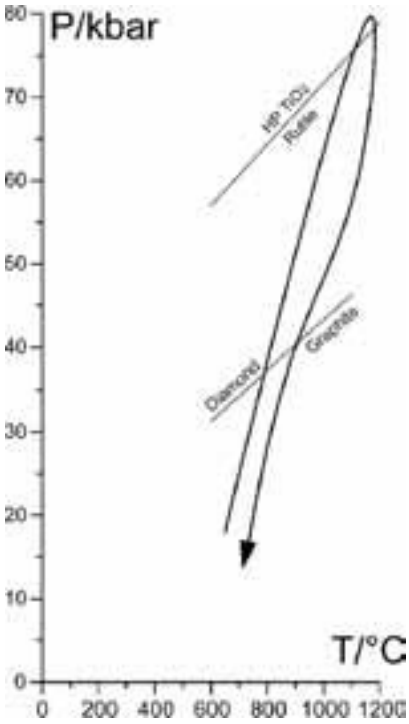

Figure 37 - P-T path derived for diamondiferous quartzofeldspathic rock from the Saidenbach reservoir, central Saxonian Erzgebirge. HP TiO_2 is TiO_2 with / -PbO_2 structure. The lower pressure limit of this phase was redetermined by Massonne et al. (2003).

of a thickened continental crust. Subsequently, the protolith was deeply subducted into the mantle to be heated to about 1200°C (Massonne, 2003). This caused considerable anatexis. The melts originated this way, still containing, for instance, garnet (cores), ascended from at least 200 km depth. Evidence for such depths is the appearance of a nanocrystal of HP TiO_2, which was found by Hwang et al. (2000) in a saidenbachite. During ascent, garnet and kyanite but also rutile, zircon, and diamond crystallised from the magma. Finally, the magma was emplaced in deep portions of thickened continental crust at P-T conditions of 15 to 18 kbar (55-60 km) and circa 750°C as determined by phengite geothermobarometry (Massonne, 1999). At this stage considerable quantities of muscovite were formed by a peritectic reaction from the remaining melt (Massonne, 2003). During the subsequent retrogression some biotite formed at the expense of muscovite. It is worthy of note that microstructural features were observed pointing to the formation of coesite, jadeitic pyroxene, and K-cymrite (Massonne,

	1	2	3	4	5	6
	E99-2a	E00-4	E98-7b	KD54	KD55	KD63
SiO2 in wt.%	64.33	69.77	59.58	74.26	71.12	74.19
TiO2	0.76	0.61	1.04	0.29	0.42	0.30
Al2O3	18.03	15.04	21.56	14.19	14.84	13.29
FeOtot	5.29	4.71	6.29	2.53	2.73	1.94
CaO	0.95	1.46	0.28	1.59	1.33	0.90
MgO	2.46	2.00	1.52	0.89	0.82	0.47
MnO	0.05	0.06	0.05	0.04	0.03	0.02
K2O	3.39	2.41	5.55	1.77	4.85	5.02
Na2O	2.51	3.23	0.37	4.28	2.92	2.51
P2O5	0.05	0.04	0.07	0.07	0.16	0.18
H2Otot	1.30	0.58	2.86	0.52	0.56	0.82
CO2	0.09	0.08	0.04	0.03	0.04	0.05
Sum	99.21	99.99	99.31	100.46	99.82	99.79
Li in ppm	100.6	100.1	65.4	120.0	42.3	76.0
Sc	20.6	15.6	6.0	9*	7.2	4.9
V (XRF)	117	89	139	32	40	25
Cr (XRF)	77	64	114	1	11	0
Ni	45.4	26.1	23.1	3.85	8.45	5.01
Cu (XRF)	17	0	19	10	0	5
Zn (XRF)	104	67	22	31	41	36
Ga (XRF)	23	19	33	19	18	19
Rb (XRF)	135	103	338	73	170	252
Sr	112	102.4	12.8	27*	112.5	84.2
Y	13.6	14.9	10.2	65.8	45.1	49.0
Zr (XRF)	167	160	103	83	190	172
Nb	13.7	12.7	19.8	6.57	11.1	14.8
Sn	1.84	2.17	34.8	8.95	2.8	4.6
Ba (XRF)	415	297	699	142	657	430
Hf/Zr	0.053	0.032	0.030		0.032	0.034
Ta	0.92	0.92	1.92	0.25	0.61	1.44
Pb	2.12	1.83	3.25	1.14	14.41	32.12
Th	2.44	6.38	4.58	0.54	12.89	16.84
U	1.23	1.82	4.30	0.10	0.77	5.42

Table 13 - XRF and ICP-MS analyses of quartzofeldspathic rocks from the GEU of the Saxonian Erzgebirge. 1,2 = diamondiferous rocks from the Saidenbach reservoir, 3 = rock without diamonds but with aspect similar to 1,2 taken northeast of the serpentinite body at Zöblitz, 4 = gneiss unusually rich in Na sampled SW of the village of Forchheim, 5,6 = ordinary gneisses taken close to diamondiferous rocks SW of Forchheim.

****=XRF data as an exception.***

2003; Massonne and Nasdala, 2003) during the ascent of the saidenbachitic magma.

The various metamorphic-magmatic stages were dated on zircons with a SHRIMP applying the U-Th-Pb-systems (Massonne et al., 2001). In addition, monazites were dated, which appear exclusively in the matrix of the saidenbachites and, thus, seem to be late stage minerals. The subsequent age data for ^{206}Pb and ^{238}U with 2$\hat{1}$ error were obtained: zircon core (dark in Fig. 36) - 336.1 ± 2.2 Ma, diamond-bearing zone (light in Fig. 36) - 336.0 ± 2.4 Ma, outer zone (very light but lacking in zircons of Fig. 36) - 329.9 ± 3.6 Ma, and monazite - 332.5 ± 3.8 Ma. Only very rare „magmatic" portions in zircon cores yielded ages as high as 396 Ma. The data of 336 Ma for the zircon cores are compatible with those around 340 Ma obtained by Kröner and Willner (1998) for gneisses of the GEU. Thus, the subsequent burial and exhumation process affecting the diamondiferous rocks took a few Ma or even less. The growth of the outermost layer of zircon and monazite formation happened some Ma after transport of the protoliths of the saidenbachites to maximum depth and also after inserting these rocks into the base of a still thickened continental crust.

Düffels and Massonne (2001) investigated the geochemical signatures of various quartzofeldspathic rocks from the GEU occurring between Saidenbach reservoir and the serpentinite body at Zöblitz (stop 3.2). Saidenbachites show clear differences from the surrounding country rocks (see, for instance, Cr, Ni, and Y of Table 13). This difference also concerns the REE patterns (Fig. 38) because all country gneisses have a very significant Eu anomaly. Thus, Düffels and Massonne (2001) disproved the idea that the saidenbachites are preserved portions of an UHP segment extending over many kilometres. It seems to be that saidenbachites and other UHP rocks form isolated bodies in rocks that had experienced, in fact, pressures as high as 20 kbar (Willner et al., 1997) but not more.

The recent investigation of the ^{13}C signature of microdiamonds in saidenbachite yielded $\delta^{13}C$(PDB)

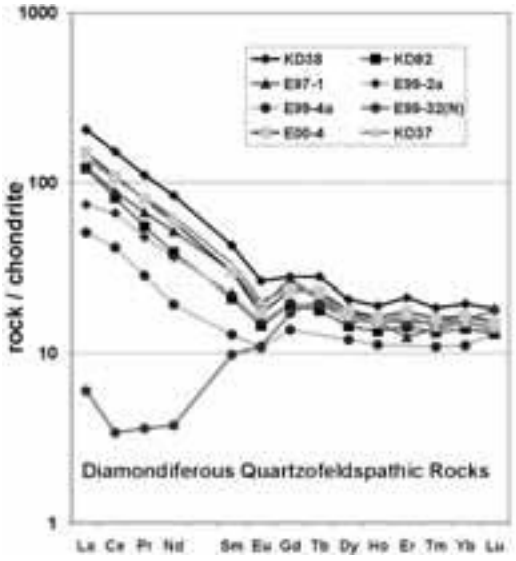

Figure 38 - REE patterns of saidenbachites from the GEU, Saxonian Erzgebirge. The data were obtained by ICP-MS analyses and subsequently normalised to chondrite. In sample E99-32(N) monazite is lacking, thus, explaining the exceptional pattern of the light REE.

values close to -30 ‰ (Massonne and Tu, 2003). This result is interpreted as an indication of an organic source of the carbon. Because bulk rock analyses of saidenbachites are very similar to those of clastic sediments (Table 13), organic material could have been already part of a sedimentary protolith. After sedimentation in Devonian times, according to the age of rare zircon cores with magmatic zonation features (Massonne et al., 2001), these rocks were deeply buried.

Stop 3.1E:

Already at the western end of the saidenbachite lens of stop 3.1D (see map of Fig. 29) but more obvious somewhat further to the southwest, blocks of quartzofeldspathic rocks appear containing cm-sized plagioclase crystals. The feldspar blastesis is interpreted as the result of an interaction of the country rocks at deep crustal levels with an alkali-rich fluid phase. The source of this phase could be the saidenbachites where it formed after the main crystallisation of the saidenbachitic magma.

Stop 3.1F:

Continuing along the strand for a few hundred metres further to the south we meet with outcropping eclogitic rocks that are virtually identical to that of stop 3.1C. Again the omphacite of the rock matrix was completely

	Gt	Omph	Phe	Gt	Phe	Phe	Phe
	core	incl.	incl.	rim	rim	core	rim
	1868/18	1868/4	1868/38	1868/24	1868/12	1771/13	1771/6
SiO_2	38.80	54.70	51.70	38.66	48.06	50.21	50.56
TiO_2	0.21	0.34	3.74	0.08	2.62	2.77	3.30
Al_2O_3	21.86	14.05	27.17	21.90	28.61	29.01	29.78
Cr_2O_3	0.00	0.00	0.08	0.06	0.05	0.00	0.01
FeO	18.60	4.06	1.72	21.96	2.36	3.10	2.60
MnO	0.37	0.02	0.04	0.53	0.00	0.01	0.01
MgO	6.93	6.95	4.06	7.84	2.74	3.35	3.21
CaO	12.63	12.57	0.01	8.50	0.00	0.00	0.00
BaO			0.36		0.18	0.20	0.20
Na_2O		6.92	0.24		0.29	0.23	0.18
K_2O			10.42		10.70	9.25	8.90
Total	99.60	99.62	99.57	99.53	95.61	98.13	97.72
Si	5.909	1.945	6.591	5.905	6.438	6.451	6.469
Al^{IV}		0.055	1.409		1.562	1.549	1.532
Ti	0.025	0.009	0.358	0.010	0.264	0.267	0.221
Al^{VI}	3.924	0.534	2.674	3.942	2.955	2.843	2.955
Cr	0.000	0.000	0.008	0.007	0.005	0.000	0.001
Fe^{3+}	0.076	0.000		0.051			
Fe^{2+}	2.319	0.121	0.184	2.754	0.264	0.333	0.278
Mn	0.047	0.001	0.005	0.069	0.000	0.001	0.001
Mg	1.573	0.368	0.777	1.785	0.548	0.641	0.611
Ca+Ba	2.061	0.479	0.019	1.382	0.010	0.010	0.016
Na		0.477	0.060		0.076	0.057	0.044
K			1.694		1.829	1.516	1.453

Table 14 - EMP analyses (in wt.%) of inclusion minerals in garnet from eclogite E42-1d as well as phengite from pegmatoid E42-1e (2 analyses on the right hand side). Both samples were taken from stop 3.1F.

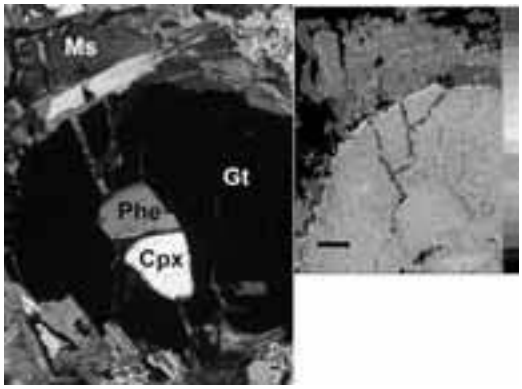

Figure 39 - Photomicrograph of a garnet (Gt) with inclusions of phengite (Phe) and omphacite (Cpx) from eclogite sample E42-1d seen under crossed polarisers. Outside garnet, muscovite (Ms) occurs. Concentration map of Mg with scale for the grey tones (increasing element concentrations towards the top) is on the right hand side. Scale bar represents 100 µm.

altered to symplectites but omphacite relics as well as phengite were found to be enclosed in garnet (Fig. 39).

Phengite geothermobarometry yielded P-T data above 30 kbar and 1000°C for the early metamorphic stage of the eclogite. In fact, no microdiamonds were found in the rock but UHP conditions or even a magmatic evolution similar to the saidenbachite cannot be excluded for this basic rock type.

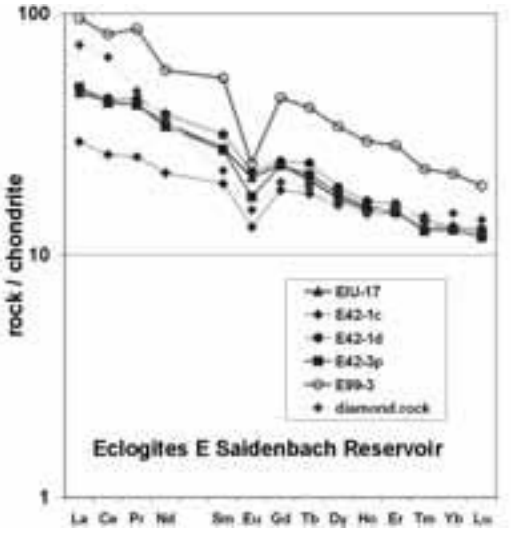

Figure 40 - REE patterns of eclogites from the eastern portion of the Saidenbach reservoir, GEU of the Saxonian Erzgebirge. The data were obtained by ICP-MS analyses and subsequently normalised to chondrite.

Volume n° 2 - from B16 to B33

	E42-1c	E42-1d	E42/2	E42-3P	EU-17	E99-3
SiO2 in wt.%	50.54	51.17	59.13	54.83	51.87	52.13
TiO2	1.78	1.57	1.43	1.75	1.87	2.45
Al2O3	15.88	16.48	17.33	16.13	17.40	16.43
FeOtot	7.48	8.24	6.96	8.13	8.81	10.78
CaO	4.73	8.78	3.81	7.21	8.02	7.91
MgO	3.66	5.56	2.13	4.56	4.97	4.45
MnO	0.14	0.14	0.11	0.13	0.15	0.19
K2O	2.40	1.46	3.54	1.80	2.11	0.74
Na2O	3.31	3.43	3.18	3.40	3.08	3.37
P2O5	0.16	0.28	0.40	0.24	0.37	0.45
H2Otot	0.92	1.42	0.72	0.79	0.67	0.61
CO2	0.18	0.30	0.21	0.20	0.23	0.18
Sum	99.18	98.83	98.95	99.17	99.55	99.65
Li in ppm	31.6	21.1		34.4	13.9	20.8
Sc	22.6	27.9	17*	23.5	24.6	27.0
V (XRF)	181	207	104	203	214	261
Cr (XRF)	98	204	47	86	124	62
Ni	21.1	38.3	17*	25.3	25.1	22.4
Cu (XRF)	36	48	28	29	29	42
Zn (XRF)	85	83	88	93	86	129
Ga	17.6	19.6	22*	21.6	19.9	19.5
Rb	46.7	34.3	69*	54.7	41.4	27.9
Sr	365	196	271*	229	290	116
Y	26.4	25.1	56*	28.8	27.4	53.8
Zr (XRF)	206	171	442	180	202	139
Nb	30.5	23.7	27*	26.7	25.7	45.7
Sn	1.03	1.07		1.88	1.16	5.85
Ba (XRF)	280	110	1304	277	402	34
Hf/Zr	0.035	0.030		0.040	0.033	0.037
Ta	2.23	1.20		1.84	1.54	5.29
Pb	10.1	1.53		4.58	2.56	8.33
Th	0.57	0.31		1.73	0.36	2.45
U	3.73	0.17		0.68	0.19	1.81

Table 15 - XRF and ICP-MS analyses of eclogites from the eastern shore of the Saidenbach reservoir, GEU of the Saxonian Erzgebirge. *=XRF data as an exception.

The geochemical characteristics of the eclogites from the eastern portion of the Saidenbach reservoir (Table 15) were studied by Massonne and Czambor (2003). The rocks are basaltic to andesitic in composition. Similar to the eclogites from the northern shore, critical parameters are: $(Nb)_N > 20$, $(Sr)_N > 10$, $Ta/Yb > 0.14$, $(La/Sm)_N = 1.2 - 2$, and $(Sm/Yb)_N > 1.4$. A further typical feature is the clear negative Eu-anomaly in all investigated samples from the eastern portion of the reservoir (Fig. 40). Protoliths of these eclogites related to magmatic rocks, for instance, from oceanic island environments cannot be excluded but sedimentary protoliths (marls) are likely, although Sc, V, Cr, and Ni contents are relatively high (see Table 15).

An interesting rock at this site is a pegmatoid forming schlieren in the eclogite body rather than a vein. It contains cm-sized phengites which have also formed in the eclogite, as quartz and feldspars, by blastesis. The composition of the phengite is given in Table 14. Phengite geobarometry yielded pressures between 18 kbar for the phengite core and 15 kbar for the rim composition at 700-750°C.

From the eclogite outcrop we walk about 400 m to the southeast to another exposure of eclogitic rocks (Fig.41).

Figure 41 - Exposure of stop 3.1G at low water level of the Saidenbach reservoir.

Stop 3.1G:

At this site however, the eclogites occur instead as bands in less basic rocks occasionally even grading into garnet-rich quartzofeldspathic rocks containing relics of kyanite. In fact, phengites have replaced kyanite, but phengite itself can be strongly altered by biotite in garnet-rich layers (Fig. 42).

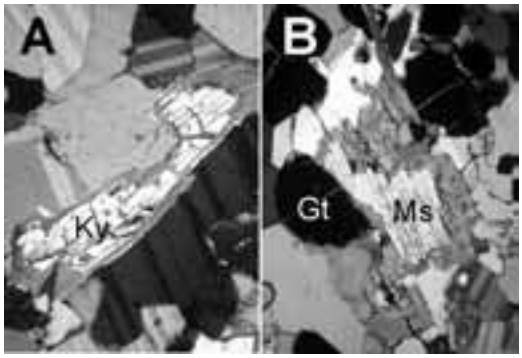

Figure 42 - Photomicrographs of objects in metapelitic sample E42/1b under crossed polarisers. A) Kyanite (Ky) relic marginally replaced by potassic white mica. Image width is 650 µm. B) Phengitic muscovite (Ms) marginally replaced by biotite. Gt = garnet. Image width is 850 µm.

From here on one could walk either back to the starting point at the road between Eppendorf and Lippersdorf or further to the east to reach after about 1.5 km the tourist parking area at the little castle of Forchheim, provided that a vehicle has been brought to this place. We practically cross the

federal road B101, heading uphill for Wernsdorf and then downhill to the Flöha valley. We cross the valley to move to Sorgau and then further to Zöblitz. Shortly after passing the town limit we must turn left to reach the entrance to the big serpentinite quarry after about 500 m. Here are parking lots on the right-hand side. The quarry is on the left-hand side (Fig. 43).

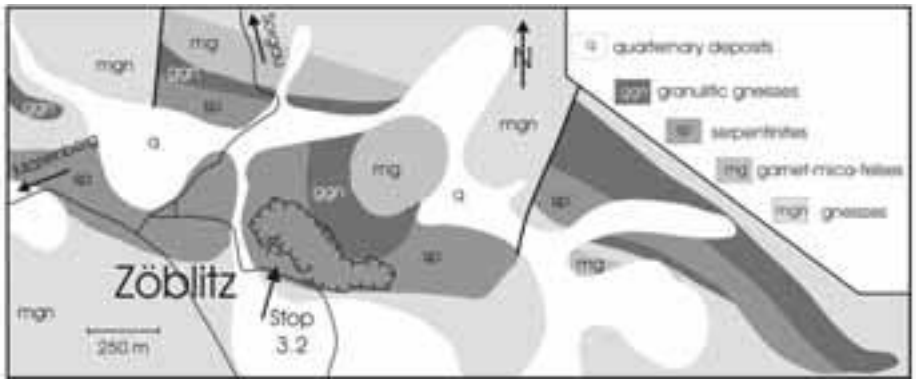

Figure 43 - Simplified geological map of the serpentinite body at the town of Zöblitz, GEU of the Saxonian Erzgebirge.

	Erz03-6d						18270			
	Gt		Opx	Cpx		Ol	Gt		Cpx	
	core	rim			rim		core	rim	core	rim
	1	6	15	20	36	40	14	140	35	136
SiO_2	42.31	42.26	57.90	54.77	54.39	40.91	39.91	40.35	53.64	51.10
TiO_2	0.66	0.63	0.14	0.41	0.44	0.02	0.57	0.25	0.48	1.03
Al_2O_3	21.92	21.83	0.98	3.72	3.47	0.00	21.97	22.72	5.45	8.61
V_2O_3	0.03	0.03	0.00	0.05	0.07	0.00	0.08	0.05	0.10	0.12
Cr_2O_3	1.60	1.67	0.14	0.92	0.85	0.00	0.01	0.05	0.32	0.04
FeO	9.00	10.06	6.49	2.61	2.58	10.15	14.72	15.91	4.79	3.50
MnO	0.33	0.41	0.11	0.07	0.06	0.09	0.27	0.30	0.02	0.00
MgO	21.31	20.47	34.96	15.52	15.69	49.14	9.19	10.35	13.25	12.93
NiO	0.00	0.00	0.06	0.01	0.02	0.37	0.00	0.00	0.00	0.00
CaO	4.26	4.47	0.39	19.61	20.49	0.00	14.81	11.48	20.16	20.40
Na_2O	0.08	0.08	0.08	2.53	2.19		0.05	0.05	2.74	2.39
K_2O				0.01	0.00		0.00	0.00	0.01	0.01
Total	101.52	101.91	101.27	100.53	100.24	100.70	101.61	101.50	100.97	100.13
Si	5.925	5.928	3.941	3.918	3.908	0.9975	5.855	5.918	3.851	3.704
Al^{IV}			0.059	0.082	0.092				0.149	0.296
Ti	0.070	0.066	0.007	0.022	0.024	0.0003	0.063	0.028	0.026	0.056
Al^{VI}	3.618	3.609	0.020	0.231	0.202	0.0000	3.799	3.927	0.312	0.440
Cr	0.177	0.186	0.008	0.052	0.048	0.0001	0.001	0.006	0.018	0.002
V	0.003	0.004	0.000	0.003	0.004	0.0001	0.009	0.006	0.006	0.007
Fe^{3+}	0.202	0.202				0.0044	0.191	0.061		
Mg	4.447	4.000	3.547	1.665	1.680	1.7659	2.009	2.262	1.418	1.397
Mn	0.039	0.048	0.006	0.004	0.004	0.0019	0.033	0.038	0.001	0.000
Fe^{2+}	0.853	0.979	0.370	0.168	0.155	0.2027	1.616	1.891	0.286	0.212
Ni	0.000	0.000	0.004	0.001	0.001	0.0072	0.000	0.000	0.000	0.000
Ca	0.640	0.672	0.028	0.001	0.001	0.0000	2.328	1.804	1.550	1.584
Na	0.022	0.021	0.011	0.350	0.305		0.014	0.006	0.382	0.335
K				0.001	0.000		0.000	0.000	0.001	0.001

Table 16 - EMP analyses (in wt.%) of minerals from serpentinised garnet lherzolite, Erz03-6d, and garnet-rich clinopyroxenite (eclogite), 18270, of the serpentinite body at the town of Zöblitz, Saxonian Erzgebirge.

Stop 3.2:

In past centuries serpentinite was quarried at Zöblitz as a rock for facing, for instance, the interior of churches and palaces. Nowadays, the main purpose of the still active quarry is to produce macadam. The serpentinite consists mainly of lizardite but clinochrysotile and antigorite are present as minor serpentine phases. In addition, aggregates of chlorite occur which are pseudomorphs after garnet. Occasionally, preserved portions of the original garnet lherzolite can be found. In such rocks garnet can form up to cm-sized crystals. As in the ultrabasic rock at Rubinberg (stop 1.2), the matrix consists of mm-sized equigranular olivine, clinopyroxene, orthopyroxene, and minor amphibole. In addition, the large extended garnet cores are chemically homogeneous. The observed fabric is interpreted as the result of recrystallisation because of deformation during the exhumation event. It started, according to the chemical composition of the matrix minerals (cores) and the garnet rim (Table 16) at P-T conditions of about 26 kbar and 1000°C applying the method reported by Massonne and Bautsch (2002). Virtually identical pressure results using the Al-content in orthopyroxene (opx) according to equilibrium (7): pyrope (in gt) = 3 $MgSiO_3$ (in opx) + Al_2O_3 (in opx). Schmädicke and Evans (1997) estimated higher pressure up to 33 kbar at temperatures somewhat below 1000°C for the garnet peridotite at Zöblitz.

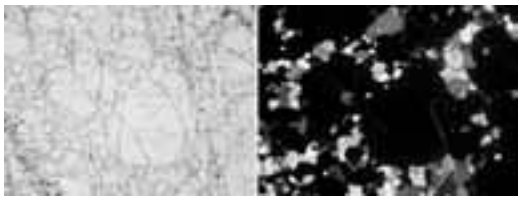

Figure 44 - Photomicrograph of garnets in clinopyroxenite (eclogite) sample 18270 under plain polarised light (left hand side) and seen under crossed polarisers (right). Image width is 4 mm.

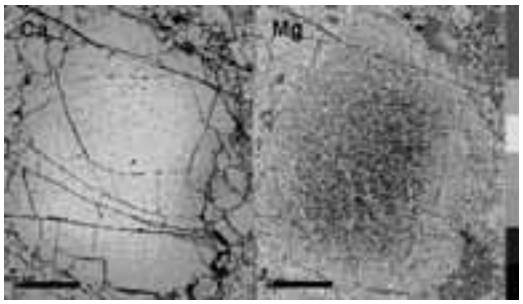

Figure 45 - Concentration maps of Ca and Mg in garnet, marginally recrystallised to garnet + clinopyroxene, in sample 18270. The scale for the grey tones shows increasing element concentrations towards the top. Scale bars represent 500 µm.

	Garnet Pyroxenites			Serpentinite
	E2b	**18270**	**E00-7B**	**E3b**
SiO_2 in wt.%	46.17	40.70	42.20	39.26
TiO_2	0.45	1.00	1.30	0.08
Al_2O_3	14.78	18.10	17.88	2.04
FeO	8.11	12.51	12.64	7.04
CaO	9.16	12.40	13.60	0.68
MgO	17.72	10.70	8.26	37.96
MnO	0.21	0.23	0.21	0.11
K_2O	0.06	0.01	0.46	0.00
Na_2O	0.85	0.17	1.08	0.00
P_2O_5	0.02	0.04	0.08	0.00
H_2O_{tot}	1.41	1.52	1.37	11.63
CO_2	0.08	0.16	0.15	0.31
Sum	99.00	97.54	99.23	99.11
Li in ppm	20.3	90.4	68.3	0.35
Sc	40.9	78.6	71.4	11.1
V (XRF)	220	402	465	51
Cr (XRF)	683	112	261	2501
Ni (XRF)	578	119	128	2350
Cu	86.2	12.5	50.5	18.6
Zn (XRF)	21	80	92	50
Ga	12.2	15.2	17.2	1.69
Rb	3.79	0.86	13.3	0.00
Sr	74.4	54.3	213	4.00
Y	13.1	22.7	25.8	1.77
Zr (XRF)	33	49	42	6
Nb	0.43	17.5	1.42	0.02
Sn	0.39	2.88	1.14	0.00
Ba	15.8	12.3	118	2.58
La	1.40	3.95	1.44	0.18
Ce	4.54	10.27	5.63	0.55
Pr	0.77	1.77	1.38	0.10
Nd	3.71	11.07	10.20	0.49
Sm	1.11	5.59	4.84	0.18
Eu	0.46	1.53	1.38	0.06
Gd	1.53	6.13	4.65	0.24
Tb	0.33	0.74	0.66	0.05
Dy	2.31	3.98	4.69	0.31
Ho	0.54	0.80	0.91	0.07
Er	1.71	2.57	2.02	0.21
Tm	0.25	0.31	0.33	0.03
Yb	1.57	2.31	2.42	0.20
Lu	0.25	0.31	0.34	0.03
Hf/Zr	0.033	0.032	0.050	0.026
Ta	1.26	1.33	0.10	0.00
Pb	0.42	2.96	37.1	1.71
Th	0.29	1.23	0.00	0.00
U	0.06	0.72	0.16	0.03

Table 17 - XRF and ICP-MS analyses of ultrabasic rocks from the serpentinite body at Zöblitz, GEU of the Saxonian Erzgebirge.

Within the peridotite body, layers of pyroxenite occur. These, when fresh, may consist mainly of clinopyroxene and garnet. Rutile is a common accessory phase. Some pyroxenites even show that up to cm-sized garnets have been marginally

transformed to smaller garnet crystals and equigranular clinopyroxene (Fig. 44). The remaining palaeocrysts are chemically zoned as shown in Fig. 45. Again, P-T conditions were determined on the basis of mineral analyses given in Table 16. For the rim composition, 16.6 kbar and 865°C were obtained. Core compositions gave much higher pressure of almost 39 kbar at 1100°C. Another possible indicator for such high or even higher pressure are abundant tiny, perfectly oriented ilmenite rods in some olivine cores of the preserved garnet lherzolite. Although no quantification in regard to the Earth's depth is possible yet, a similar exsolution feature, e.g. reported by Green et al. (1997) from the peridotite massif of Alpe Arami, was taken as a hint at UHP conditions. Summarizing the petrological information on the ultrabasic body at Zöblitz, it can be concluded that the exhumation history is virtually the same as for the ultrabasic rocks from the nearby Granulitgebirge.

Geochemical analyses of garnet pyroxenites from Zöblitz (Table 17) show that these rocks can vary significantly in composition. The garnet lherzolite (Table 17) is somewhat depleted in light REE.

From the serpentinite quarry we go to the centre of the town of Zöblitz to meet with federal road B171 heading to Marienberg and then on to Wolkenstein. After passing this town we reach federal road B101. From here it is as far as 9 km to the town of Annaberg-Buchholz.

DAY 4

The excursion continues from Annaberg-Buchholz via federal road B95 to the south reaching Hammerunterwiesenthal after 17 km. In the centre of this village we turn right heading uphill to Neudorf. Close to the Hammerunterwiesenthal exit a dirt road on the left leads to "Steinbruchbetriebe Richter".

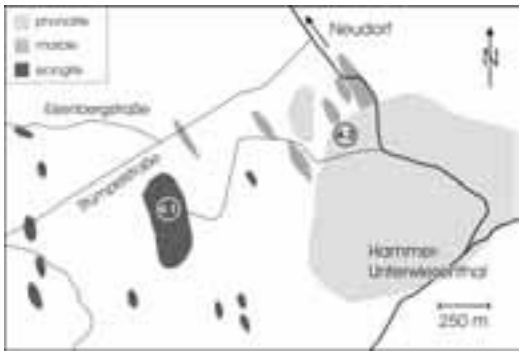

Figure 46 - Simplified geological map of an area in the MEU of the Saxonian Erzgebirge close to the village of Hammerunterwiesenthal.

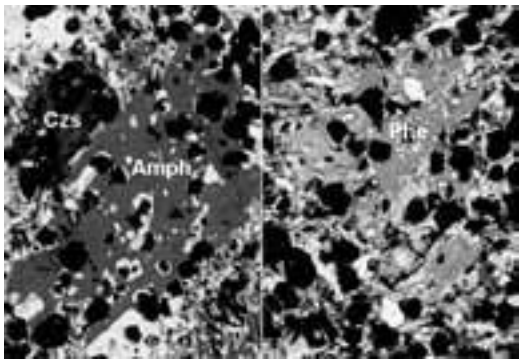

Figure 47 - Photomicrographs of porphyroblasts of amphibole (Amph), clinozoisite (Czs), and phengite (Phe) in eclogite 18333 (stop 4.1) under crossed polarisers. Image width is 900 µm each.

Here it is possible to talk to the owner of the eclogite quarry. This quarry, however, can be reached by taking the next dirt road to the left. This road ends at the eclogite quarry after about 1.3 km (Fig. 46).

Stop 4.1

At this stop we can visit what is left of a lens of homogeneous eclogite about 500 m long. In spite of the destruction of a formerly romantic site in the wood, as the Stümpelfelsen cliffs were considered, the relationships to the gneissic country rocks are well exposed now.

In fact, the eclogites at the Stümpelfelsen can be distinguished by lighter and darker varieties, but they are all massive and not as foliated as other eclogites in the vicinity. Another common aspect is produced by mm long, non-oriented amphibole crystals in a relatively fine-grained matrix consisting mainly of fresh omphacite and garnet (Fig. 47). A few larger single white mica flakes are also discernible with the naked eye in the common eclogite. In addition, several mm-sized amphiboles and oriented white mica flakes can be strongly enriched on mm thick planes often between eclogite and quartz segregations crosscutting the eclogite body. Also crosscutting are cracks, occasionally running parallel with dm spacings, along which late retrograde minerals, such as chlorite and actinolite, have formed. These caused a darker colouring in the mm range around the cracks.

In the light coloured variety the eclogitic mineral assemblage is characterised by garnet, omphacite, phengite, talc, amphibole, clinozoisite, quartz, rutile, and accessory phases. At a late stage (III) of metamorphism porphyroblasts of amphibole, clinozoisite, and phengite formed. Paragonite joined the assemblage even during a later stage

Mineral	Gt		Omph		Amph		Czs		Talc	Phe		Parag
Stage	Ib	II-IIIa	I-II	II-III	Ib	IIIa	Ib	IIIa	IIIa	Ib-II	IIIa	IIIb
SiO_2 in wt.%	38.94	39.34	56.26	56.12	56.79	54.66	37.94	39.31	62.46	53.47	52.46	47.40
TiO_2	0.11	0.08	0.04	0.06	0.05	0.13	0.14	0.12	0.02	0.23	0.28	0.07
Al_2O_3	21.75	22.06	9.15	10.57	3.13	8.69	29.03	31.11	0.43	26.90	28.20	39.41
Cr_2O_3	0.04	0.03	0.09	0.07	0.03	0.02	0.06	0.08	0.01	0.02	0.11	0.06
Fe_2O_3							6.15	3.33				
FeO	25.27	24.23	3.33	3.62	5.73	6.98			4.38	1.48	1.48	0.48
MnO	1.12	0.82	0.04	0.07	0.10	0.09	0.10	0.04	0.00	0.00	0.00	0.00
MgO	3.41	5.77	10.09	8.85	20.15	16.35	0.18	0.12	28.33	4.52	3.89	0.27
CaO	11.40	9.82	15.36	13.76	11.25	7.80	23.70	24.52		0.01	0.01	0.28
Na_2O	0.02	0.04	5.62	6.66	1.48	3.96	0.00	0.04	0.09	0.53	0.84	6.83
K_2O					0.07	0.12				10.34	9.53	0.99
BaO					0.00	0.00				0.24	0.19	0.00
Sum	102.06	102.19	99.98	99.78	98.76	98.80	97.12	98.68	95.72	97.73	96.99	95.83
Si	5.982	5.946	2.001	1.993	7.736	7.457	2.959	2.993	4.009	6.886	6.786	6.016
Ti	0.013	0.009	0.001	0.002	0.005	0.013	0.008	0.007	0.001	0.022	0.027	0.007
Al	3.939	3.929	0.384	0.443	0.502	1.397	2.668	2.791	0.033	4.088	4.299	5.895
Cr	0.005	0.003	0.003	0.002	0.003	0.003	0.004	0.005	0.001	0.002	0.011	0.007
Fe^{3+}	0.056	0.067	0.000	0.024	0.331	0.313	0.361	0.191				
Fe^{2+}	3.190	2.994	0.099	0.083	0.322	0.484			0.235	0.160	0.160	0.051
Mn	0.145	0.104	0.001	0.002	0.011	0.010	0.007	0.003	0.000	0.000	0.000	0.000
Mg	0.780	1.299	0.535	0.469	4.091	3.324	0.021	0.014	2.711	0.868	0.751	0.051
Ca	1.877	1.589	0.585	0.524	1.641	1.140	1.985	2.000	0.011	0.001	0.001	0.038
Na	0.007	0.013	0.391	0.459	0.390	1.046	0.000	0.006		0.132	0.212	1.680
K					0.012	0.021				1.702	1.572	0.161
Ba					0.000	0.000				0.012	0.011	0.000

Table 18 - EMP analyses (in wt.%) of minerals from eclogite 18333 sampled at the Stümpelfelsen cliff (stop 4.1), MEU of the Saxonian Erzgebirge. The data were taken from Massonne and Kopp (submitted).

(IIIb). The chemical zonation of the minerals are exemplary shown by Figs. 48 to 50 and Table 18. On the basis of this, various geothermobarometric methods were applied considering phengite and talc strongly. The constrained P-T path for the eclogite starts at about 480°C and 25 kbar (stage Ib in Fig. 51) followed by a significant temperature increase (stage II) at slightly increasing pressures. At the peak P-T conditions of 720°C and 27 kbar

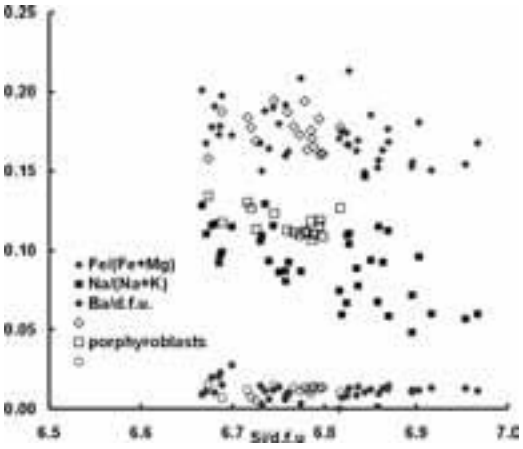

Figure 48 - Compositional variation of phengite as small grains of the matrix and as porphyroblasts in eclogite 18333 from the Stümpelfelsen cliff close to the village of Hammerunterwiesenthal.

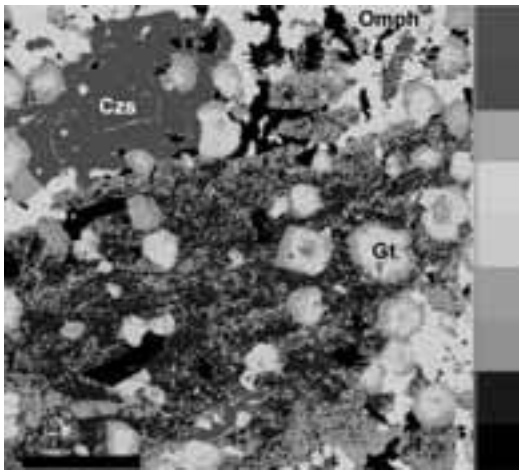

Figure 49 - Concentration map of Ca for a section of sample 18333 with an amphibole and clinozoisite (Czs) porphyroblast also shown on the left hand side of Fig. 47. Several grains enclosed in amphibole are garnet (Gt). Outside the porphyroblast is omphacite (Omph). The scale for the grey tones shows increasing element concentrations towards the top. Scale bar represents 250 µm.

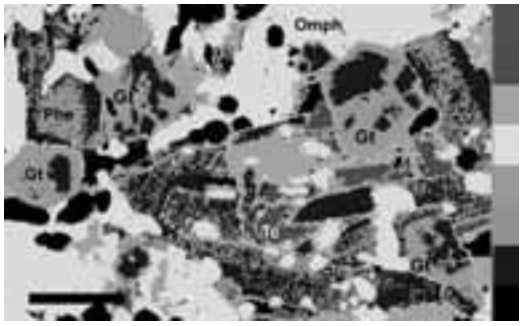

Figure 50 - Concentration map of Mg for a matrix section of eclogite sample 18333 from the Stümpelfelsen cliff close to the village of Hammerunterwiesenthal. Gt = garnet, Omph = omphacite, Phe = phengite, Tc = talc. The scale for the grey tones shows increasing element concentrations towards the top. Scale bar represents 100 µm.

	1	2	3	4	5	6
SiO2 in wt.%	49.04	50.58	50.64	49.74	66.76	71.68
TiO2	1.99	1.61	1.56	1.37	0.12	0.16
Al2O3	13.79	13.66	14.48	13.92	19.51	16.39
FeOtot	12.80	11.55	9.80	10.25	0.28	0.25
CaO	10.36	10.61	11.21	10.68	1.03	1.28
MgO	6.39	6.54	7.20	6.92	0.32	0.21
MnO	0.25	0.24	0.18	0.16	0.01	0.01
K2O	0.61	0.90	0.21	0.25	0.64	3.48
Na2O	2.17	2.66	2.89	2.99	10.63	5.75
P2O5	0.14	0.09	0.11	0.08	0.39	0.13
H2Otot	1.35	1.42	0.26	1.29	0.43	0.56
CO2	0.01	0.03	0.11	0.33	0.17	0.06
Sum	98.90	99.89	98.85	97.96	100.29	99.96
Li in ppm	10.6	20.8	35.8	23.3		25.4
Sc	46.2	36.9	46.0	47.6	3*	0.50
V (XRF)	378	343	350	320	10	21
Cr (XRF)	214	185	289	357	21	0
Ni	62.1	55.5	46.5	52.5	1*	0.0
Cu (XRF)	38	12	17	17	1	3
Zn (XRF)	112	130	128	87	6	6
Ga	14.9	14.2	14.0	15.2	15*	13.4
Rb	48.4	59.1	11.1	6.11	29*	64
Sr	72	54	156	98	49*	471
Y	49.4	43.0	45.2	44.7	16*	1.24
Zr (XRF)	100	81	90	74	52	86
Nb	1.60	2.03	1.89	1.72	9*	1.45
Sn	1.06	2.78	23.9	10.7		0.66
Ba (XRF)	47	170	22	29**	20	806
Hf/Zr	0.045	0.040	0.048	0.062		0.026
Ta	0.21	0.20	0.27	0.19		0.0
Pb	6.91	2.95	0.73	1.36		31.51
Th	0.14	0.12	0.33	0.27		2.99
U	0.03	0.16	0.06	0.05		1.76

*Table 19 - XRF and ICP-MS analyses of eclogites from the MEU of the Saxonian Erzgebirge. 1 (E96-15b) and 2 (E96-15d) = stop 4.1, 3 (E22a) and 4 (E22c) = stop 4.3 Analyses 5 and 6 represent small volumes of rocks, either with pegmatoid or granitoid character, directly in contact to eclogites. 5 (Erz03-4) = stop 4.3, 6 (E42-1e) = stop 3.1F. *=XRF data as an exception.*

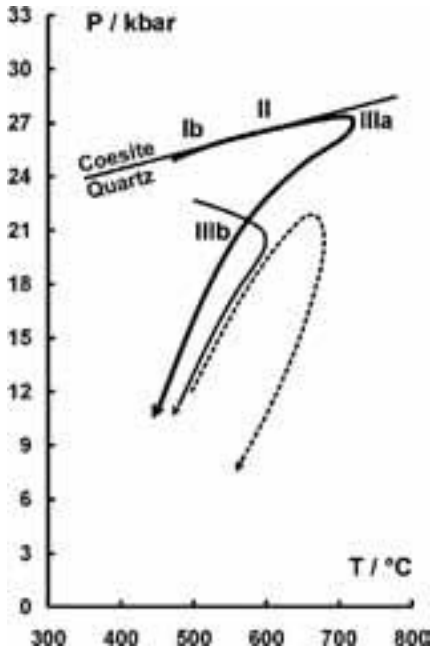

Figure 51 - P-T paths derived for low-temperature eclogites from the MEU of the Saxonian Erzgebirge. Bold: eclogite from stop 4.1. Roman numbers refer to metamorphic stages. Medium line: eclogite taken a few kilometres north of the town of Marienberg (Massonne, 1992). Dashed: eclogites of the MEU, in general, according to Schmädicke et al. (1992).

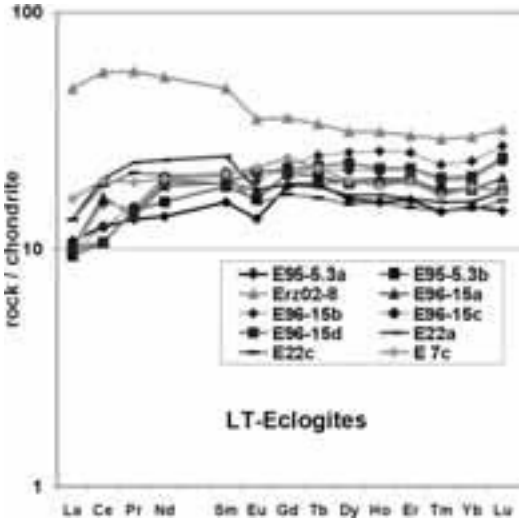

Figure 52 - REE patterns of eclogites from the western Erzgebirge´s crystalline massif. However, samples Erz02-8 and E7c were taken a few kilometres north and east, respectively, of the town of Marienberg. The data were obtained by ICP-MS analyses and subsequently normalised to chondrite.

porphyroblasts began to grow by invading hydrous fluids. Possibly the resulting density reduction caused buoyancy forces uplifting the eclogite. Subsequently, significant cooling occurred at still high pressures. Stage IIIb is characterised by P-T conditions around 520°C and 18 kbar at reduced water activities. This unusual late P-T history might explain the freshness of the eclogite including the preservation of chemical zonation on the micrometer scale.

The geochemical characteristics of eclogites from the MEU was investigated by Massonne and Czambor (2003). Among the analysed samples were those from the Stümpelfelsen cliff (Table 19). These eclogites could be assigned to former MORBs demonstrated, for instance, by the REE patterns of these rocks (Fig. 52).

In the quarry of stop 4.1 the typical country rocks are outcropping as well. These are quartz-rich gneisses, probably former greywackes, and mica schists occasionally with large garnets several mm in diameter. The latter rock type, which can also contain chloritoid, was studied by Rötzler et al. (1998). These authors estimated P-T conditions of 12 kbar and 525°C for the pressure climax as well as 8 kbar and 560°C for the subsequent temperature peak. These P-T data differ significantly from those derived for the eclogites. Willner et al. (2000, 2002) tried to explain this by a model involving rapid exhumation of high-pressure rocks from the root zone of a collisional orogen. Unfortunately, it is not clear yet, if the low-temperature eclogites of the western Erzgebirge were metamorphosed at the same time as those of the central Erzgebirge. Schmädicke et al. (1995) also determined ages as old as 355 Ma for the eclogites from the western Erzgebirge. If there is really a considerable time difference between metamorphism of (U)HP rocks from the western and central Erzgebirge, a single major event responsible for the exhumation of these rocks has to be called into question.

On the way back to the main road, we stop after about 1 km at the entrance to a larger, apparently abandoned quarry on the left-hand side (see Fig. 46).

Stop 4.2: (optional)

In this quarry we can see a good example for one of the many alkali-dominated subvolcanics which erupted in the Tertiary. In fact, this type of volcanism concentrated in the Eger-graben to the south, but there are quite a number of such stocks penetrating the crystalline massif of the Erzgebirge. Another reason to visit this quarry is a marble with some siliceous layers (Fig. 53) in the northern portion of the quarry. Such marbles form elongated bodies similar to those of the nearby eclogites. It is also obvious

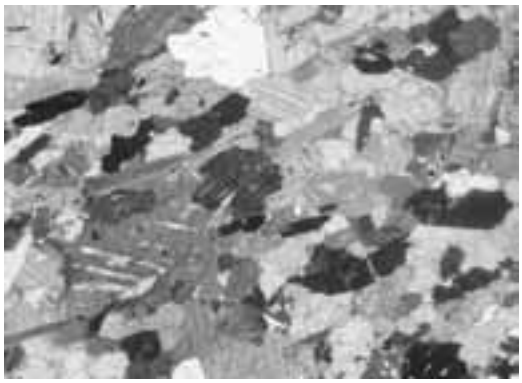

Figure 53 - Photomicrograph of a siliceous layer in marble from stop 4.2 seen under crossed polarisers. The silicates are amphibole and phlogopite. Image width is 4 mm

that both rock types marbles and eclogites are associated over a wide area, but a real contact between both does not exist. It is also not clear what the P-T conditions of the metamorphism of the marble were. The common mineral assemblage amphibole, clinopyroxene, and phlogopite with carbonates in particular does not allow to quantify pressure conditions.

After going back to the main road we turn left to reach the village of Neudorf after 4 km. Just after crossing the railroad track, we turn left heading for the forester´s house "Siebensäure". After 1.8 km, we pass this building to park our vehicle(s) on the left-hand side. As the road is closed to the public, we have to walk further to the west by about 600 m. Then we turn right into the forest. Already after some tens of metres cliffs occur which extend for a few hundred metres in a northwest direction.

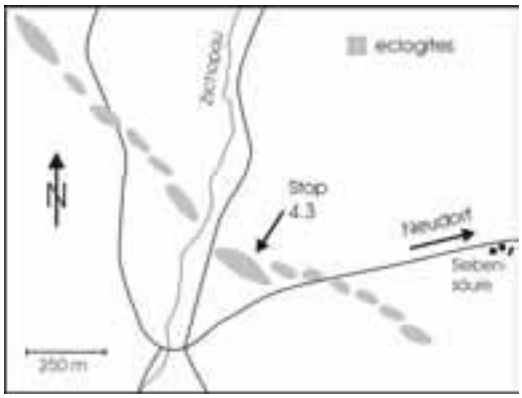

Figure 54 - Simplified geological map of an area in the MEU of the Saxonian Erzgebirge a few kilometres west of the village of Neudorf.

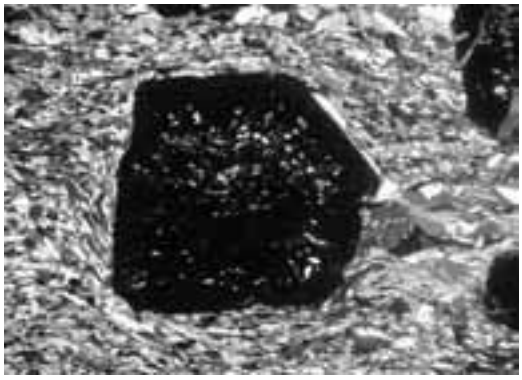

Figure 55 - Photomicrograph of a large garnet, seen under crossed polarisers, in a foliated matrix of sample E22h from stop 4.3. The matrix consists mainly of amphibole and clinozoisite. Image width is 4 mm.

At the end, another paved forest road appears.

Stop 4.3:

The cliffs in the forest consist of eclogites which form either a larger strongly elongated lens or, as shown on the map of Fig. 54, a number of smaller lenses. In fact, the eclogite of stop 4.3 is geochemically identical to that of stop 4.1 (see Table 19), but here it is, as typical for the western Erzgebirge, clearly

	Gt		Omph		Phe	
	core	rim	core	rim	core	rim
	988/52	988/85	988/7	988/22	988/32	988/25
SiO_2	37.88	38.97	55.14	56.68	53.67	52.60
TiO_2	0.12	0.03	0.04	0.02	0.22	0.27
Al_2O_3	21.14	21.91	6.66	10.13	26.75	28.82
Cr_2O_3	0.00	0.00	0.04	0.05	0.00	0.02
FeO	26.44	22.91	7.27	3.01	1.50	1.47
MnO	2.26	0.23	0.06	0.04	0.00	0.00
MgO	4.22	8.17	9.55	9.62	4.49	3.90
CaO	8.11	7.94	15.58	14.85	0.00	0.00
BaO					0.10	0.34
Na_2O	0.02	0.01	5.47	5.85	0.52	0.76
K_2O			0.02	0.03	11.04	10.81
Total	100.20	100.17	99.84	100.08	98.28	98.79
Si	5.925	5.918	1.992	2.001	6.919	6.751
AlIV			0.008	0.000	1.081	1.249
Ti	0.015	0.003	0.001	0.001	0.022	0.026
AlVI	3.898	3.921	0.276	0.421	2.983	3.110
Cr	0.000	0.000	0.001	0.001	0.000	0.002
Fe^{3+}	0.102	0.079	0.112	0.000		
Fe^{2+}	3.357	2.831	0.108	0.089	0.162	0.158
Mn	0.299	0.029	0.002	0.001	0.000	0.000
Mg	0.985	1.849	0.514	0.506	0.862	0.746
Ca+Ba	1.359	1.291	0.603	0.554	0.005	0.017
Na			0.383	0.426	0.131	0.188
K			0.001	0.001	1.815	1.737

Table 20 - EMP analyses (in wt.%) of minerals in eclogite E22h taken from stop 4.3.

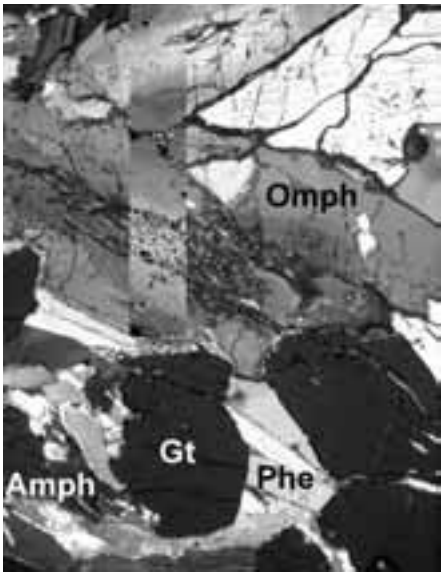

Figure 56 - Photomicrograph of a preserved portion of palaeocrysts in eclogite E22h seen under crossed polarisers. The superposed inlet is a concentration map showing rising Fe contents by increasingly lighter grey tones. Image width is 2.7 mm.

foliated. Occasionally, we can find in the cliffs of stop 4.3 a preserved fabric in the cm range, formed before deformation. In these preserved portions, mm-sized garnet and omphacite occur (Figs. 55 and 56). These minerals are strongly chemically zoned. From the core compositions of these minerals and a relatively coarse-grained phengite (see Table 20) about 24 kbar and 500°C were calculated for an early metamorphic stage. Rim compositions yielded 26 kbar and 650°C. The resulting P-T path resembles that obtained for eclogites from stop 4.1. Formation of amphibole and clinozoisite, from which the fine-grained foliated matrix mainly consists of, as well as deformation happened at the P-T climax and/or during the beginning of exhumation.

An interesting feature in the outcrop are granite-like segregations at the contact between eclogite and country rock. The composition of this granitoid is characterised by high Na_2O (> 10 wt.%, see Table 19) and, thus, high plagioclase contents. The same is true for similar segregations in the serpentinite body at Zöblitz and to some extent for the pegmatoid schlieren in eclogite of stop 3.1F (Table 19). However, no genesis model can be currently presented.

After going back to Neudorf, we take the road to the left and turn after a few hundred metres slightly to the left heading for Crottendorf and the village of Scheibenberg which we reach after 8 km. We

Volume n° 2 - from B16 to B33

Figure 57 - Columns of nephelinite at Scheibenberg hill.

turn right into federal road B101, pass the village, and, at its exit, turn left heading for Zwönitz and further to Stollberg. Do not forget to have a look at the so-called "Orgelpfeifen" (Fig. 57) when leaving Scheibenberg. This natural monument consists of great vertical columns of nephelinite which intruded the Erzgebirge's crystalline massif during Tertiary times as well. The columns are still discernible although relatively far away.

After reaching Stollberg we turn north before entering the centre of the town. About 2 km north of Stollberg there is access to highway A72 heading for Chemnitz. At the northwestern edge of this city is the junction for highway A4 heading for Dresden. This city is reached after about 70 km.

Acknowledgements

Research in the Saxonian Erzgebirge, which contributed to a significant portion of this guide, was founded by Deutsche Forschungsgemeinschaft (project No. Ma1160/2 and Ma 1160/19). Thomas Theye and Andreas Brandelik supported our electron microprobe work, calculations of structural formulae, and preparation of some figures.

References

Blümel, P. (1995). V. Saxothuringian Basin C. Exotic metamorphic nappes 2. Metamorphic evolution. In "Pre-Permian geology of central and eastern Europe" (Dallmeyer, R.D., Franke, W. and Weber, K., Eds.), Springer Verlag, Berlin, 295-308.

Chopin, C. (1984). Coesite and pure pyrope in high grade blueschists of the Western Alps: a first record and some consequences. Contributions to Mineralogy and Petrology 86, 107-118.

Chopin, C. (2003). Ultrahigh pressure metamorphism: tracing continental crust into the mantle. Earth and Planetary Science Letters 212, 1-14.

Dobrzhinetskaya, L.F., Schweinehage, R., Massonne, H.-J. and Green, H.W. II (2002). Silica precipitates in omphacite from eclogite at Alpe Arami, Switzerland: Evidence of deep subduction. Journal of metamorphic Geology 20, 481-492.

Düffels, K. and Massonne, H.-J. (2001). Geochemical signatures of diamondiferous gneisses and their adjacent rocks from the Erzgebirge, Germany. Terra Nostra, 5/2001, 24-26.

Franke, W. (2000). The mid-European segment of the Variscides: tectonostratigraphic units, terrane boundaries and plate tectonic evolution. In "Orogenic Processes: Quantification and Modelling in the Variscan Belt" (Franke, W., Haak, V., Oncken, O. and Tanner, D., Eds.), Geological Society of London, Special Publication 179, 35-61.

Franke, W. and Engel, W. (1986): Synorogenic sedimentation in the Variscan belt of Europe. Bulletin Soc. geol. France 1986 II, 25-33.

Franke, W. and Stein, E. (2000). Exhumation of high-grade rocks in the Saxo-Thuringian Belt: geological constraints and geodynamic concepts. In "Orogenic Processes: Quantification and Modelling in the Variscan Belt" (Franke, W., Haak, V., Oncken, O. and Tanner, D., Eds.), Geological Society of London, Special Publication 179, 337-354.

Green, H.W. II, Dobrzhinetskaya, L., Riggs, E.M. and Jin, Z.-M. (1997). Alpe Arami: a peridotite massif from the Mantle Transition Zone? Tectonophysics 279, 1-21.

Hartz, E.H. and Torsvik, T.H. (2002). Baltica upside down: A new plate tectonic model for Rodinia and the Iapetus Ocean. Geology 30, 255-258.

Hwang, S.-L., Shen, P., Chu, H.-T. and Yui, T.-F. (2000). Nanometer-size α-PbO_2-type TiO_2 in garnet: a thermobarometer for ultrahigh-pressure metamorphism. Science 288, 321-324.

Jekosch, U. and Bautsch, H.-J. (1991). Orientierte Entmischungen in Pyroxenen. Zeitschrift für Kristallographie, Supplement, 4, 134.

Kröner, A. and Willner, A.P. (1998). Time of formation and peak of Variscan HP-HT metamorphism of quartz-feldspar rocks in the central Erzgebirge, Saxony, Germany. Contributions to Mineralogy and Petrology 132, 1-20.

Krohe, A. (1996). Variscan tectonics of central Europe: Postaccretionary intraplate deformation of weak continental lithosphere. Tectonics 15, 1364-1388.

Massonne, H.-J. (1992). Thermochemical determination of water activities relevant to eclogitic rocks. In "Water-rock interaction WRI-7" (Kharaka, Y.K. and Maest, A., Eds.), Proceedings of the 7th International Symposium, Park City, Utah, U.S.A., 2, 1523-1526.

Massonne, H.-J. (1994). P-T evolution of eclogite lenses in the crystalline complex of the Erzgebirge, Middle Europe: An example for high-pressure to ultrahigh-pressure metabasites incorporated into continental crust. First Workshop on UHP metamorphism and tectonics, Stanford University, Abstract Volume, A29-A32.

Massonne, H.-J. (1999). A new occurrence of microdiamonds in quartzofeldspathic rocks of the Saxonian Erzgebirge, Germany, and their metamorphic evolution. Proceedings of the 7th International Kimberlite Conference, Cape Town 1998, P.H. Nixon Volume, 533-539.

Massonne, H.-J. (2001). First find of coesite in the ultrahigh-pressure metamorphic region of the Central Erzgebirge, Germany. European Journal of Mineralogy 13, 565-570.

Massonne, H.-J. (2003). A comparison of the evolution of diamondiferous quartz-rich rocks from the Saxonian Erzgebirge and the Kokchetav Massif: are so-called diamondiferous gneisses magmatic rocks? Earth and Planetary Science Letters 216, 347-364.

Massonne, H.-J. (in press). Paläozoische Hochdruck- und Ultrahochdruck-Metamorphite in Mitteleuropa und ihre Beziehungen zur variszischen Orogenese. Zeitschrift für geologische Wissenschaften.

Massonne, H.-J. and Burchard, M. (2000). Exotic minerals in eclogites from the Central Erzgebirge – evidence for fluid-rock interaction at UH metamorphic pressures: Berichte der deutschen mineralogischen Gesellschaft, Beihefte zum European Journal of Mineralogy 12, No. 1, 122.

Massonne, H.-J., Dobrzhinetskaya, L. and Green, H.W. II, (2000). Quartz - K-feldspar intergrowths enclosed in eclogitic garnet and omphacite. Are they pseudomorphs after coesite? Extended Abstract, 31st International Geological Congress, Rio de Janeiro, Brazil: 4 pp. (on CD, search for Massone).

Massonne, H.-J., Nasdala, L. and Kennedy, A. (2001). U-Th-Pb dating of zircons and monazites from diamondiferous gneisses of the Saxonian Erzgebirge – implications for their UHP/HP evolution. 6th International Eclogite Conference, Niihama, Japan, Abstract Volume, 88.

Massonne, H.-J. and Bautsch, H.-J. (2002). An unusual garnet pyroxenite from the Granulitgebirge, Germany: origin in the transition zone (>400 km Earth's depths) or in a shallower upper mantle region? International Geology Reviews 44, 779-796.

Massonne, H.-J., Bautsch, H.-J., Kopp, J. and Theye, T. (2002). Enigmatic origin of syenite boudins in a serpentinite from the Variscan Granulitgebirge, Germany. 18th General Meeting of the International Mineralogical Association, Edinburgh 2002, Abstract Volume, 216.

Massonne, H.-J. and Bautsch, H.-J. (2003). P-T evolution of a spinel-garnet-bearing clinopyroxenite from the Granulitgebirge. Berichte der deutschen mineralogischen Gesellschaft, Beihefte zum European Journal of Mineralogy 15, No. 1, 127.

Massonne, H.-J., Burchard, M., Frost, D. and Theye, T. (2003). Thermodynamic properties of TiO_2 with / -PbO_2 structure based on HP experiments. Berichte der deutschen mineralogischen Gesellschaft, Beihefte zum European Journal of Mineralogy 15, No. 1, 128.

Massonne, H.-J. and Czambor, A. (2003). Protoliths of eclogites from the Variscan Erzgebirge. Norges geologiske undersøkelse Report 2003.055, Eclogite Field Symposium, Abstracts, 93-94.

Massonne, H.-J. and Nasdala, L. (2003). Characterization of an early metamorphic stage through inclusions in zircon of a diamondiferous quartzofeldspathic rock from the Erzgebirge, Germany. American Mineralogist 88, 883-889.

Massonne, H.-J. and O'Brien, P.J. (2003). The Bohemian Massif and the NW Himalaya. In "Ultrahigh Pressure Metamorphism" (Carswell, D.A. and Compagnoni, R., Eds.), EMU Notes in Mineralogy 5, 145-187.

Massonne, H.-J. and Tu, W. (2003). δ^{13}C-Signature of microdiamonds from the Saxonian Erzgebirge, Germany. Norges geologiske undersøkelse Report 2003.055, Eclogite Field Symposium, Abstracts, 91-92.

Massonne, H.-J. and Kopp, J. (submitted). A low-variance mineral assemblage with talc and phengite in an eclogite from the Saxonian Erzgebirge, Middle Europe, and its P-T evolution. Journal of Petrology.

Matte, P. (1986): Tectonics and plate tectonics model for the Variscan belt of Europe. Tectonophysics 126, 329-374.

Matte, P. (1998). Continental subduction and exhumation of HP rocks in Paleozoic orogenic belts: Uralides and Variscides. Geologiska Föreningens Stockholm Förhandlingar 120, 209-222.

McKerrow, W.S., Mac Niocaill, C., Ahlberg, P.E., Clayton, G., Cleal, C.J. and Eagar, R.M.C. (2000). The Late Palaeozoic relations between Gondwana and Laurussia. In „Orogenic Processes: Quantification and Modelling in the Variscan Belt" (Franke, W., Haak, V., Oncken, O. and Tanner, D., Eds.), Geological Society of London, Special Publication 179, 9-20.

Murphy, J.B., Keppie, J.D., Dostal, J. and Nance, R.D. (1999). Neoproterozoic - early Paleozoic evolution of Avalonia. In "Laurentia-Gondwana connections before Pangea" (Ramos, V.A. and Keppie, J.D., Eds.), Geological Society of America, Special Papers 336, 253-266.

Nasdala, L. and Massonne, H.-J. (2000).

Volume n° 2 - from B16 to B33

Microdiamonds from the Saxonian Erzgebirge, Germany: in situ micro-Raman characterisation. European Journal of Mineralogy 12, 495-498.

O'Brien, P.J. (2000). The fundamental Variscan problem: high-temperature metamorphism at different depths and high-pressure metamorphism at different temperatures. In "Orogenic Processes: Quantification and Modelling in the Variscan Belt" (Franke, W., Haak, V., Oncken, O. and Tanner, D., Eds.), Geological Society of London, Special Publication 179, 369-386.

Oliver, G.J.H., Corfu, F. and Krogh, T.E. (1993). U-Pb ages from SW Poland: evidence for a Caledonian suture zone between Baltica and Gondwana. Journal of the Geological Society of London 150, 355-369.

Reiche, M. and Bautsch, H.-J. (1984). Entmischungsstrukturen in Pyroxenen aus eklogitischen Gesteinen. Freiberger Forschungshefte C393, 19-33.

Reiche, M. and Bautsch, H.-J. (1985). Electron microscopical study of garnet exsolution in orthopyroxene. Physics and Chemistry of Minerals 12, 29-33.

Reinhardt, J. and Kleemann, U. (1994). Extensional unroofing of granulitic lower crust and related low-pressure, high-temperature metamorphism in the Saxonian Granulite Massif, Germany. Tectonophysics 238, 71-94.

Robardet, M., Paris, F. and Racheboeuf, P.R. (1990). Palaeogeographic evolution of southwestern Europe during Early Palaeozoic times. In "Paleozoic paleogeography and biogeography" (McKerrow, W.S. and Scotese, C.R., Eds.), Geological Society of London Memoirs 12, 411-419.

Romer, R.L. and Rötzler, J. (2001). P-T-t evolution of ultrahigh-temperature granulites from the Saxon Granulite Massif, Germany. Part II: Geochronology. Journal of Petrology 42, 2015-2032.

Rötzler, J. and Romer, R.L. (2001). P-T-t evolution of ultrahigh-temperature granulites from the Saxon Granulite Massif, Germany. Part I: Petrology. Journal of Petrology 42, 1995-2013.

Rötzler, K., Schumacher, R., Maresch, W.V. and Willner, A.P. (1998). Characterization and geodynamic implications of contrasting metamorphic evolution in juxtaposed high-pressure units of the Western Erzgebirge (Saxony, Germany). European Journal of Mineralogy 10, 261-280.

Schmädicke, E., Okrusch, M. and Schmidt, W. (1992). Eclogite-facies rocks in the saxonian Erzgebirge, Germany: high pressure metamorphism under contrasting P-T-conditions. Contributions to Mineralogy and Petrology 110, 226-241.

Schmädicke, E., Cosca, M.A. and Okrusch, M. (1995). Variscan Sm-Nd and Ar-Ar ages of eclogite facies rocks from the Erzgebirge, Bohemian Massif. Journal of Metamorphic Geology 13, 537-552.

Schmädicke, E. and Evans, B.W. (1997). Garnet-bearing ultramafic rocks from the Erzgebirge, and their relation to other settings in the Bohemian Massif. Contributions to Mineralogy and Petrology 127, 57-74.

Schulmann, K., Ledru, P., Autran, A., Melka, R., Lardeaux, J.M., Urban, M. and Lobkowicz, M. (1991). Evolution of nappes in the eastern margin of the Bohemian Massif: a kinematic interpretation. Geologische Rundschau 80, 73-92.

Stampfli, G. (1996). The intra-Alpine terrain: a palaeotethyan remnant in the Alpine Variscides. Eclogae Geol. Helvetiae 89, 12-42.

Stampfli, G.M., von Raumer, J. and Borel, G.D. (2002). Paleozoic evolution of pre-Variscan terranes: From Gondwana to the Variscan collision. In "Variscan-Appalachian Dynamics: The Building of the Late Paleozoic Basement" (Martínez Catalán, J.R., Hatcher, R.D. Jr., Arenas, R. and Díaz García, F., Eds.), Geological Society of America, Special Papers 364, 263-280.

Stöckhert, B., Duyster, J., Trepmann, C. & Massonne, H.-J. (2001): Microdiamond daughter crystals precipitated from supercritical COH silicate fluids included in garnet, Erzgebirge, Germany. Geology 29, 391-394.

Tait, J., Bachtadse, V. and Soffel, H.C. (1994). Silurian paleogeography of Armorica: new paleomagnetic data from Central Bohemia. Journal of Geophysical Research 99, 2897-2907.

Tait, J., Schätz, M., Bachtadse, V. and Soffel, H. (2000). Palaeomagnetism and Palaeozoic palaeogeography of Gondwana and European terranes. In "Orogenic Processes: Quantification and Modelling in the Variscan Belt" (Franke, W., Haak, V., Oncken, O. and Tanner, D., Eds.), Geological Society of London, Special Publication 179, 21-34.

Willner, A.P., Rötzler, K. and Maresch, W.V. (1997). Pressure-temperature and fluid evolution of quartzo-feldspathic metamorphic rocks with a relic high-pressure, granulite-facies history from the Central Erzgebirge (Saxony, Germany). Journal of Petrology 38, 307-336.

Willner, A.P., Krohe, A. and Maresch W.V. (2000). Interrelated P-T-t-d paths in the Variscan Erzgebirge dome (Saxony, Germany): Constraints on the rapid

Back Cover:
field trip itinerary

FIELD TRIP MAP

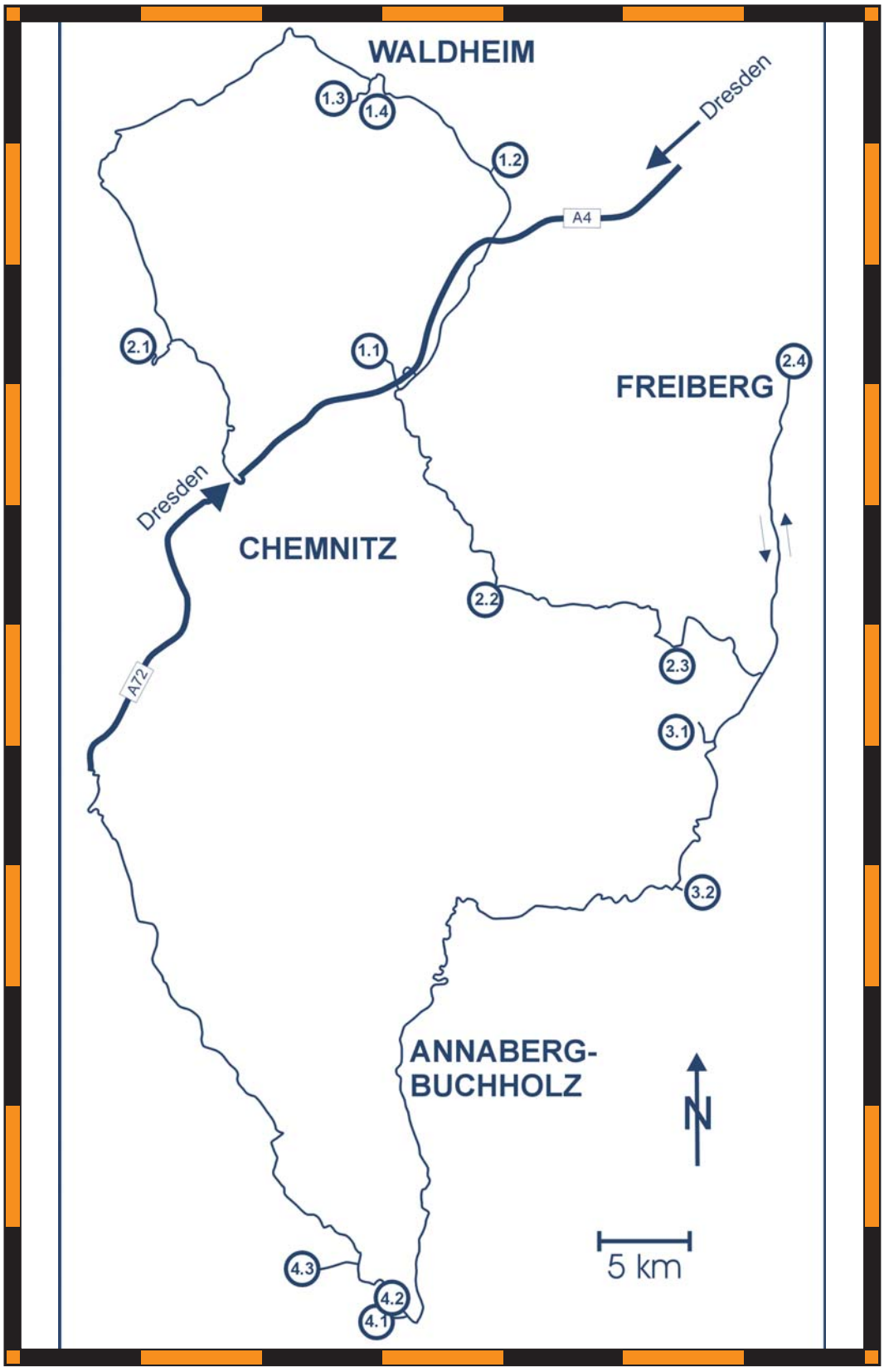

32nd INTERNATIONAL GEOLOGICAL CONGRESS

Edited by APAT